RESEARCH ARTICLE | JULY 07 2023

A perspective on metallic liquids and glasses

K. F. Kelton

Journal of Applied Physics 134, 010902 (2023)
https://doi.org/10.1063/5.0144250

Journal of Applied Physics PERSPECTIVE pubs.aip.org/aip/jap

A perspective on metallic liquids and glasses

Cite as: J. Appl. Phys. **134**, 010902 (2023); doi: 10.1063/5.0144250
Submitted: 28 January 2023 · Accepted: 8 June 2023 ·
Published Online: 7 July 2023

K. F. Kelton[a)]

AFFILIATIONS

Department of Physics and the Institute of Materials Science and Engineering, Washington University, St. Louis, Missouri 63130, USA

[a)]**Author to whom correspondence should be addressed:** kfk@wustl.edu

ABSTRACT

Metallic glasses have the potential to become transformative materials, but this is hindered by the lack of ability to accurately predict which metallic alloys will form good glasses. Current approaches are limited to empirical rules that often rely on parameters that are unknown until the glasses are made, rendering them not predictive. In this Perspective, properties of metallic liquids at elevated temperatures and how these might lead to better predictions for glass formation are explored. A central topic is liquid fragility, which characterizes the different dynamics of the liquids. What fragility is and how it might be connected to the liquid structure is discussed. Since glass formation is ultimately limited by crystallization during cooling, recent advances in crystal growth and nucleation are also reviewed. Finally, some approaches for improving glass stability and glass rejuvenation for improved plasticity are discussed. Building on a summary of results, some key questions are raised and a prospective for future studies is offered.

I. INTRODUCTION

Over the past two to three decades, metallic glasses have been increasingly recognized as promising technological materials. Their superior soft magnetic properties, which were quickly recognized after their discovery, led to applications in electrical transformer cores.[1] Their high strength, hardness, and corrosion and abrasion resistance are ideal for coating applications[2,3] and biomedical materials.[4,5] They are being considered for additional applications that range from electrode materials for electro-catalytic degradation of water contaminants[6] to improved biosensors.[7] While metallic glasses tend to be brittle, limiting their uses as structural materials, recent advances have led to glasses with increased plasticity.[8–10] In some cases, this has been achieved by controlled crystallization,[11] a technique widely used to prepare technologically important silicate glass ceramics.[12,13] A truly unique feature among metals is the ability for metallic glasses to be thermoformed. This grew out of pioneering work on extrusion, showing superplastic deformation at high strain rates,[14] injection molding,[15] hot rolling,[16] and blow molding.[17] Thermoforming allows the production of precision components that can replicate micrometer and smaller features,[18] create surfaces that are smooth to an atomic level,[19] and enable nanofabrication by molding.[20] Stretch blow molding, with strains exceeding 2000% (compared to 150% for blow molding) promises to greatly extend the fabrication range of possible parts and geometries.[21]

Despite their demonstrated promise, metallic glasses have not yet realized their full potential. To do so requires an ability to (i) increase the number of metallic glasses that can be tailored to specific applications (currently they are only found in a few alloy families), (ii) produce glasses of a sufficiently large physical size (the first metallic glasses could only be formed as very thin ribbons), and (iii) make glasses that are stable against crystallization for a sufficiently long time (this is a problem for many non-metallic glasses as well, particularly those used in pharmaceuticals).[22] These points are the goals of active international research. Identifying good glass forming liquids remains largely a laborious trial and error approach, although there are some guidelines that can be followed[23–25] and the search can be assisted by using combinatorial approaches.[26,27] Machine learning techniques have also been investigated,[28–30] but a recent study raises questions about their validity for identifying good glass formers.[31] Recently, it has been suggested that clues for metallic glass formation can be found in the properties of high temperature liquids.[32,33]

This article focuses on a few key areas: (i) the properties of metallic liquids at elevated temperatures and how these might influence glass formation, (ii) methods used to identify good glass forming metallic alloys, (iii) an examination of key processes that prevent glass formation from the supercooled liquid, such as crystallization, and the (iv) question of glass stability. The first question focuses on possible relations between the structure and dynamics

in metallic liquids. The second gives a sense of what has been used and what is being developed to lead to improved search methods for new metallic glass. The third point focuses on the processes of crystal nucleation and growth. As will be discussed, there are recent studies that raise questions about the classical theories of these processes. Since glass formation ultimately hinges on avoiding significant crystallization during cooling, improved insight into these processes could play a key role in predicting glass formation. The final focus is on glass stability, which is also relevant for crystallization, but additionally depends on relaxation processes in the glass that can alter the glass dynamics. The primary goal is to provide a perspective into these developing areas, identify some key questions, and explore directions that future work might follow. While background information is essential and is provided, no attempt is made for this to be comprehensive.

II. METALLIC LIQUIDS

Before beginning a discussion of how properties of metallic liquids might aid in identifying good glass formers, it is useful to make some general comments about the structure and dynamics of liquids. The structure of a liquid is considerably less well understood than are the structures of crystals and gases. Crystals contain both short-range and extended periodic or quasi-periodic long-range order, interrupted only locally by defects such as vacancies, stacking faults, and grain boundaries. In contrast, at sufficiently high temperature, a gas has no structure, although some short-range order can develop at lower temperatures. Liquids fall in between these extremes, having significant short-range order, but which extends to only a few neighbors away. Furthermore, it is difficult to say what the "structure" of a liquid really means, since it is inherently time dependent. The time scales for structural dynamics are on the order of pico-seconds (ps). In a metallic solid, collective excitations called phonons interact with processes such as electrons, leading to a temperature-dependent electrical resistivity. In metallic liquids, however, the phonons are overdamped and often localized, which may play a role in understanding some recent measurements that show an apparent temperature independent plateau in the electrical resistivity at high temperatures.[34] This will be discussed in Sec. II C.

The recently developed ability to process liquids in a high vacuum environment without the need for a container and the introduction of high intensity synchrotron x-ray and spallation neutron facilities have led to more accurate measurements of static and time-dependent liquid structures and the viscosity at high temperature. Coupled with classical and *ab initio* molecular dynamics studies, these new experimental data are leading to a reconsideration of how structure and dynamics are related. But before discussing the structural and dynamical data, it is useful to give a brief introduction to the levitation techniques used. A detailed discussion and comparison of different techniques can be found elsewhere.[35,36]

A. Containerless processing

Traditionally, the dynamical, thermodynamic, and structural properties of metallic liquids were measured while holding the liquid in a container. This significantly limited the temperature range and the types of liquid that could be studied, since many metallic liquids react with their containers at elevated temperatures. Recent advances in containerless processing using aerodynamic/acoustic,[37,38] electromagnetic (EML),[35] and electrostatic (ESL)[39,40] levitation techniques have greatly expanded the systems and temperature ranges that can be explored. Containerless facilities (EML and ESL) are also available on the International Space Station (see chapters 3 and 5 in Ref. 41).

Samples can be processed under a high vacuum in both EML and ESL, making these particularly useful for studying reactive metallic liquids at high temperatures. Each has their advantages and failings. Levitation is achieved in EML by passing radio frequency (RF) current through a coil that surrounds the sample. This induces eddy currents in metallic samples, creating a counter magnetic field that causes the sample to levitate. The eddy currents also heat and can even melt the samples. However, because heating and positioning are coupled, dense samples with low liquidus temperatures must be processed in a gas environment to achieve significant cooling. This problem is largely avoided with the EML facility in the European rack on the International Space Station (ISS-EML),[42–44] since very little force is required to levitate samples in a microgravity environment. In ESL, samples are levitated in a strong electrostatic field; they are heated and melted using a high-power laser (often a solid-state laser). Sample positioning is more difficult in ESL, since unlike EML there is no stable minimum in the field. Instead, the sample is backlit, using either cross-polarized lasers or high-power diodes of different colors that are located at 90° to each other, and the shadow of the sample is measured by two position sensitive detectors (PSD) placed in line with the source of backlighting to determine the location of the sample at any time. Based on the sample position, an appropriate voltage is applied to electrodes to keep the sample at the desired location. Since heating and positioning are decoupled, ESL allows processing to lower temperatures without the need for a gas environment. However, it is only possible to process samples that have a small evaporation rate over the temperature range of interest, which is not as significant an issue with EML.

Thermophysical and dynamical properties, such as the density, surface tension, and viscosity, and the maximum supercooling for crystal nucleation can be measured in EML[45–52] and ESL.[53–65] Both have been used to determine liquid structures as a function of temperature from X-ray[56,66–75] and elastic neutron[76–81] scattering studies. The diffusion coefficients in the liquid have been determined from quasi-elastic neutron scattering measurements.[82,83] Recently, the first measurements of the time-dependent liquid structure of a metallic liquid at high temperature were made using the Neutron ESL (NESL) facility located at the Spallation Neutron Source (SNS).[84] Finally, a new feature of the ISS-EML allows measurements of the electrical resistance of metallic liquids to very high temperatures.[85] The results from scattering, viscosity, and resistivity measurements form a significant part of the backbone of this Perspective.

B. Liquid viscosity—A measure of the dynamics

Dynamical processes in liquids are traditionally inferred from the shear viscosity, η. The viscosities of liquids change by over 16

orders of magnitude from their value at the melting (or liquidus) temperature, T_ℓ, to the glass transition temperature, T_g (the temperature at which the liquid becomes a glass). The precise nature of the glass transition remains an unsolved problem, despite years of investigation and many proposed explanations. This is not discussed here; reviews can be found elsewhere.[86–90]

1. Fragility

The glass transition temperature, T_g, is conventionally defined as the temperature where the shear viscosity, η, of the liquid is 10^{13} poise (equal to 10^{12} Pa s). Differences between different liquid families are apparent when $\log(\eta)$ is graphed as a function of the inverse temperature multiplied by T_g (i.e., T_g/T).[91] Angell characterized the different behavior in terms of the liquid's *fragility*. At sufficiently elevated temperatures, the temperature dependence of the viscosity for all liquids is approximately Arrhenius, i.e., $\eta \propto \exp(-Q/k_BT)$, where Q is an activation energy, T is the temperature in absolute units, and k_B is the Boltzmann constant. The activation energy is equal to the slope in the graph of $\log(\eta)$ vs T_g/T. For some liquids, such as SiO_2 (Fig. 1), the viscosity remains Arrhenius with a constant activation energy as the temperature is decreased to T_g; these are called *strong* liquids. For *fragile* liquids, such as o-terphenyl (Fig. 1), the activation energy is small at high temperatures but increases rapidly upon approaching T_g (this is called "super-Arrhenius" behavior). Angell defined the fragility factor, m, from the slope near the glass transition temperature, T_g,

$$m = \frac{d\log\eta}{d(T_g/T)}\Big|_{T=T_g}. \quad (1)$$

This quantity increases with the fragility of the liquid. For liquids shown in Fig. 1, m is largest for one of the most fragile liquids, o-terphenyl, and is smallest for SiO_2. For metallic glasses (illustrated by $Zr_{41.2}Ti_{13.8}Cu_{12.5}Ni_{10}Be_{22.5}$), m (and hence the fragility) falls between these two extremes.

Within the metallic glass community, fragility is often associated with glass formability,[94–97] making it a parameter of considerable practical as well as fundamental importance. The association is reasonable, since stronger liquids tend to have a larger viscosity at higher temperatures leading to decreased crystal nucleation and growth rates (which ultimately determine glass formation, see Sec. III B). However, this is not universal; sorbitol and salol are very fragile liquids that form glasses.[98] Furthermore, studies show that in metallic liquids, factors other than fragility must be considered to develop a better understanding of glass formation.[97] The microscopic origins of fragility remain uncertain, despite studies spanning over several decades. As will be discussed, many factors approximately correlate with fragility but never perfectly. Considering the amount of research on fragility over many years without the development of an understanding of underpinnings of the quantity, it may be that fragility is an incomplete concept. Nevertheless, it is useful to look at microscopic properties that may contribute to fragility.

From the conventional definition of the glass transition temperature discussed previously, the viscosities of all liquids will be equal at T_g. A universal extrapolated value of the viscosity at infinite temperature, η_o, has been argued for metallic liquids[99] and silicate glasses.[100] Many theoretical expressions have been proposed to describe the viscosity as a function of temperature (see Ref. 99 for a list). However, the most commonly used is the phenomenological Vogel–Fulcher–Tammann (VFT) expression,[101–103]

$$\eta = \eta_o \exp\left(\frac{B}{T - T_o}\right), \quad (2)$$

where B is a constant and T_o is the low temperature at which in this expression the viscosity diverges in VFT. While first proposed as a phenomenological relation, justification has been made within the configurational entropy[104,105] and free volume[106–108] models.

By fitting Eq. (2) to the viscosity at high temperatures, a fragility strength parameter, D^* [$=B/T_o$ in Eq. (1)] can be related to the fragility defined at T_g,

$$m = m_{\min} + \frac{m_{\min}^2 \ln(10)}{D^*}. \quad (3)$$

Although it is widely used, the VFT fits poorly to the measured viscosities of metallic liquids, and the strength parameter can become unphysical,[109] so this approach should be used with caution. A different high temperature approach does not suffer from this issue. As is evident in Fig. 1, the magnitude of the viscosity at elevated temperatures tends to be larger for stronger liquids.

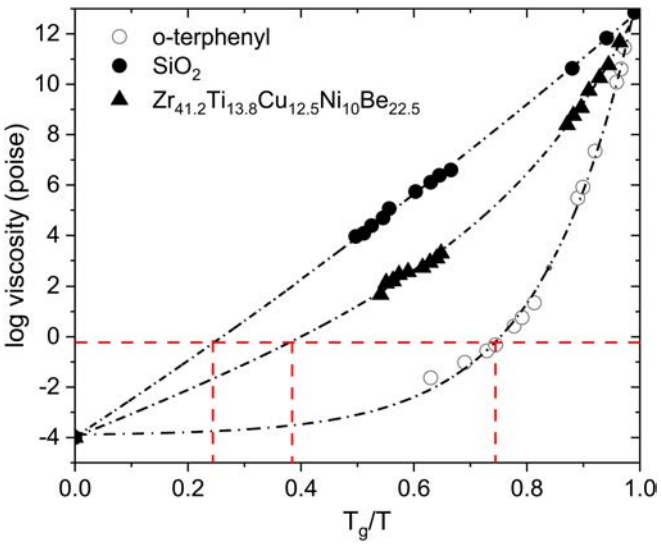

FIG. 1. Measured viscosities for SiO_2 (a strong liquid), ortho terphenyl (a fragile liquid) (both from Ref. 92) and a metallic glass, which is of intermediate fragility (from Ref. 93). Since T_g is defined as the temperature where the viscosity equals 10^{13} poise (10^{12} Pa s), all of the viscosity curves meet at that point. They also tend to a constant value at infinite temperature (where $T_g/T = 0$). The dashed horizontal line corresponds to a common viscosity of 0.6 poise. The vertical dashed lines correspond to the value of a quantity T_g/T^*, which is larger for more fragile liquids.

Based on this, Angell argued that the temperature, $T_{1/2}$, where the log of the viscosity is midway between η_o and the value at T_g, could be used as a measure of fragility, i.e., $F_{1/2}$,[110]

$$F_{1/2} = 2\,\frac{T_g}{T_{1/2}} - 1\,. \tag{4}$$

There is nothing unique about this choice, however. Any common value of the viscosity that intersects all of the dataset will work. A new fragility index, T_g/T^*, can, therefore, be defined for the high temperature liquid, where T^* is the temperature at which the liquids have the same viscosity.[111] As shown in Fig. 1, stronger liquids have smaller values of T_g/T^*.

While fragility has historically been defined in terms of viscosity (kinetic fragility), it is also manifest in other liquid properties, such as the entropy[112] and specific heat,[113] and in the Poisson ratio[114] and the bulk modulus[115] in glasses. This suggests that there may be a connection between the dynamics (viscosity) and the amorphous structure. In fact, the terms fragile and strong were based on an assumption of how the liquid structure changed near T_g.[91] Angell argued that when a glass that is formed from a strong liquid is heated above T_g, the liquid maintains the more locally ordered structure of the glass until the temperature becomes too high. For a glass formed from a fragile liquid, however, the liquid quickly "forgets" the ordered glass structure on heating above T_g. The results of experimental studies support these assumptions, as will be discussed in Sec. II G.

2. The onset of cooperativity

Molecular dynamics studies have identified a temperature, T_A, where liquid dynamics become cooperative.[116] The viscosity has an Arrhenius temperature dependence with a constant activation energy above T_A. The activation energy is related to the energy required to change the coordination number of a local cluster by one, defined to be a structural excitation. Above T_A, the lifetime of the excitation is so short that nearest neighbors cannot receive information of the excitation (by pseudo-phonon—henceforth called phonon—exchanges) in time to respond to it. With decreasing temperature, however, the time for the change in local configuration becomes longer, comparable to the phonon lifetime, so below T_A, neighboring atoms can respond to local excitations and the dynamics become cooperative. Increasingly, more atoms interact cooperatively as the temperature is decreased, causing the activation energy to increase and giving super-Arrhenius behavior, as can be observed in Fig. 1. Experimental data obtained from containerless studies of a large number of metallic liquids support the MD predictions. If the viscosities measured at high temperatures near T_A are normalized to the extrapolated value of the viscosity at infinite temperature, η_o, and the inverse temperature is normalized to T_A, the data collapse onto one curve (Fig. 2). The data shown are from several different alloy families, suggesting that this might be universal behavior for all metallic alloy liquids. Since this has been experimentally investigated by only one research group,[99] however, studies by others and in other metallic liquids are needed for verification.

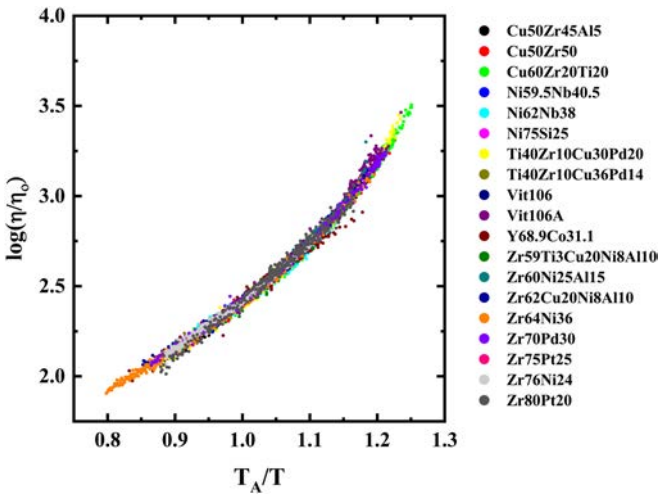

FIG. 2. The viscosity measured at high temperatures using the modulation technique in electrostatic levitation[117] for several metallic alloy liquids collapsed onto a universal curve for log (η/η_o) as a function of T_A/T. Reproduced from Blodgett *et al.*, Sci. Rep. **5**, 13837 (2015).[99] Copyright 2015 Author(s), licensed under a Creative Commons Attribution 4.0 License.

Techniques allow the viscosity of metallic liquids to be measured near the liquidus temperature and at low temperatures near the glass transition temperature. Since few measurements exist in the mid-temperature range, however, it is necessary to extrapolate between these limits using an analytical expression. As mentioned earlier, the most commonly used of these and the least accurate is the Vogel–Fulcher–Tammann expression. Other, more accurate, functions are listed in Table I of Ref. 99 One of these (KKZNT) assumes a geometrically frustrated avoided critical point at a temperature T^* that corresponds closely with T_A,

$$\log(\eta/\eta_o) = \frac{1}{T}(E_\infty + T^* B[(T^* - T)/T^*]^z\,\Theta(T^* - T)), \tag{5}$$

where $\Theta(x)$ is the Heaviside function and $z \approx 8/3 \pm 1/3$.[86,118,119] Based on a fit to the viscosity data for Vit 106a ($Zr_{57}Cu_{15.4}Ni_{12.6}Al_{10}Nb_5$), E_∞ and B were determined and then held constant for all other metallic liquids; η_o and T^* (T_A) were determined from the viscosity data for each metallic liquid. As shown in Fig. 3, the same universal curve was obtained for all of the viscosity data at high and low temperatures. The Vit 1 ($Zr_{41.2}Ti_{13.8}Ni_{10}Cu_{12.5}Be_{22.5}$) viscosity data appear to deviate slightly from the universal curve, possibly due to a liquid/liquid phase transition that causes an abrupt change in the fragility,[120] as will be discussed later. These fits were only made for metallic liquids. A more recent study, however, has presented a universal form for the viscosity that fits metallic and silicate glasses.[121]

Experimental studies show that T_A correlates with T_g, with $T_A \simeq 2T_g$ for metallic liquids.[99] A different ratio (T_A/T_g) is found for non-metallic glasses.[122] It has also been argued that T_g/T_A correlates with fragility,[123] with stronger liquids having smaller values

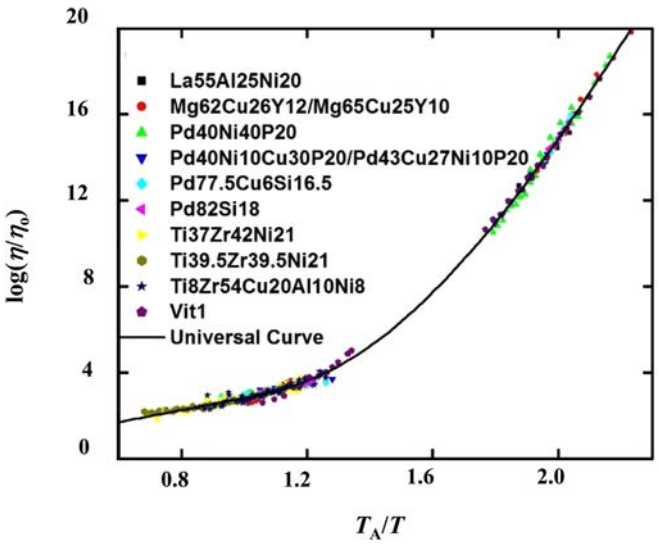

FIG. 3. Literature values for the viscosity measured at high and low temperatures for several metallic alloy liquids collapsed onto a universal curve for log (η/η_o) as a function of T_A/T. The solid black line is a fit to the avoided critical point (KKZNT) model for the viscosity. Reproduced from Blodgett *et al.*, Sci. Rep. **5**, 13837 (2015).[99] Copyright 2015 Author(s), licensed under a Creative Commons Attribution 4.0 License.

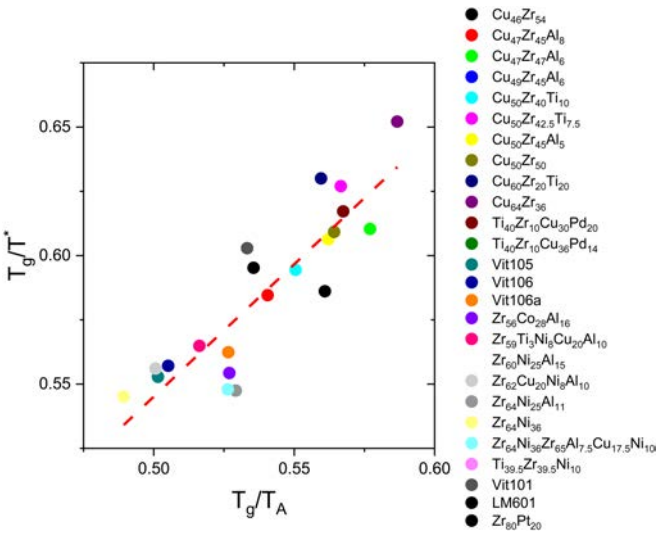

FIG. 4. The correlation between T_g/T^* and T_g/T_A. As shown in Fig. 3 of Ref. 111, T_g/T^* correlates with the fragility parameter, m. This plot shows that T_g/T_A also correlates with m (since it correlates with T_g/T^*). (Data taken from Ref. 32.)

of T_g/T_A. In agreement, a survey of 20 metallic liquid compositions shows a strong correlation between T_g/T^* and T_g/T_A (Fig. 4).

C. Electrical resistivity of metallic liquids at high temperatures

The expression commonly used to describe the electrical resistivity, ρ, of amorphous metals (liquids or glasses) was developed in the 1960s.[124–127] It is calculated from the X-ray structure factor, $S(q)$, which provides a measure of the static structure of the liquid (see Sec. II E),

$$\rho(T) = \frac{3\pi\Omega}{4\hbar e^2 v_F^2 k_F^4} \int_0^{2k_F} S(q, T)\ |u(q)|^2\ q^3 dq, \tag{6}$$

where Ω is the atomic volume, $\hbar$ is Planck's constant divided by 2π, e is the electronic charge, v_F is the Fermi velocity, k_F is the Fermi momentum, q is the momentum transfer, and $u(q)$ is the pseudopotential. Since the integral in Eq. (6) is heavily weighted for large q, ρ can be approximated as

$$\rho(T) \propto\ S(2k_F, T)\,|u(2k_F)|^2. \tag{7}$$

Because electrons scatter strongly from the structure, an examination of the resistivity as a function of temperature might give structural evidence for the onset of cooperativity at T_A. Measurements made using a facility on the International Space Station[85] confirm this (Fig. 5), with the temperature dependence of

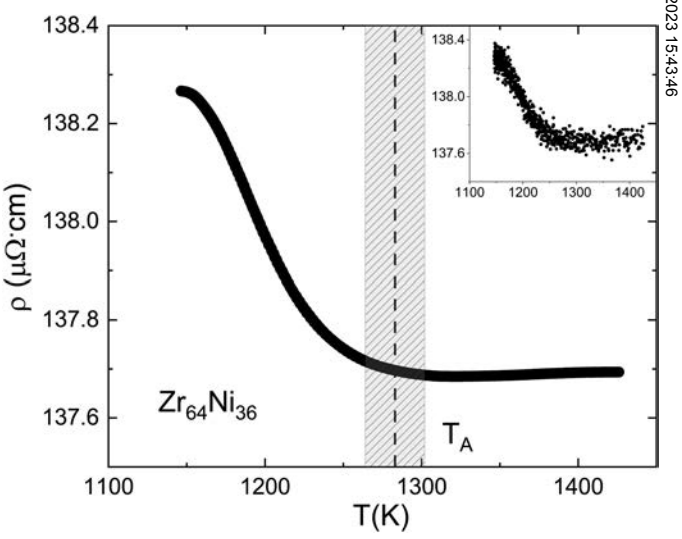

FIG. 5. Electrical resistivity of liquid $Zr_{64}Ni_{36}$ as a function of temperature. Smoothed data are shown in the main figure; the unsmoothed data are shown in the inset in the upper right-hand corner of the figure. The bounds on the measured T_A are shown in the gray hatched region. On approaching T_A, the temperature coefficient becomes small and vanishes above T_A as the resistivity enters a plateau. Reproduced with permission from Van Hoesen *et al.*, Phys. Rev. Lett. **123**, 226601 (2019).[34] Copyright 2019 the American Physical Society.

the resistivity of liquid $Zr_{64}Ni_{36}$ changing markedly at T_A. This provides strong evidence for a structural change at T_A that corresponds to the dynamical changes, as predicted from MD simulations. Additional evidence will be found in the time-dependent pair distribution, the Van Hove function, as discussed in Sec. II H.

Most surprising is that above T_A, the resistivity becomes essentially constant as a function of temperature, indicating that electron–phonon scattering is no longer effective. This plateau has also been observed in liquid $Cu_{50}Zr_{50}$[34] and in $Zr_{80}Pt_{20}$ and $Pt_{57.5}Cu_{14.7}Ni_{5.3}P_{22.5}$,[128] suggesting that it could be a universal feature. While such plateaus have been observed at cryogenic temperatures due to electron localization, to my knowledge this is the first plateau observed in a liquid at high temperatures. The plateaus cannot be explained by Eq. (6) since x-ray measurements demonstrate that $S(q)$ shows no discontinuous change at or above T_A. One suggestion is that above a characteristic temperature, assumed to be T_A, the mean electron scattering time becomes comparable to the lifetime of local structural excitations, decreasing the effectiveness of electron–phonon scattering.[34] However, even at T_A, the structural excitation lifetime is several orders of magnitude longer than the electron scattering time. While at this time a clear explanation for the plateau is lacking, it appears evident that a new theory of electrical resistivity in metallic liquids is required.

D. Liquid/Liquid phase transitions and fragility

Liquid/Liquid (LL) phase transitions have been observed in several liquids, including water,[129] an Al_2O_3-Y_2O_3 liquid,[130] metal-organic-framework liquids,[131] and several metallic liquids[132,133] and glasses.[134–136] The nature of LL transitions is still hotly debated. In some cases, they occur at temperatures above the liquidus temperature, close to the expected values for T_A,[133,137,138] suggesting that they might be a crossover instead of an actual phase transition. In other cases, they occur at much lower temperatures, $\sim 1.2T_g$,[139] suggesting that they could be associated with mode coupling. In some cases, these LL transitions have been attributed to fragile-strong (FS) transitions, from a fragile liquid at high temperature to a strong liquid at low temperature. Computer simulations predict FS transitions in SiO_2[140] and BeF_2[141] and LL transitions that might be connected to FS transitions in Si[142] and C.[143]

Following Angell's definition of fragility, FS transitions in metallic liquids and glasses are typically inferred from the temperature dependence of the viscosity.[120,139,144–146] In these cases, the extrapolation of the viscosity at high temperature fails to match the values measured at low temperatures. In most cases, however, the extrapolation between high and low temperature is made using the configurational entropy (MYEGA) expression.[100] While this gives a much better fit to viscosity data than the commonly used VFT expression [Eq. (2)], it does not provide a good fit for metallic liquids.[99] How much this influences the conclusion of a FS transition should be investigated, for example, using the avoided critical point (KKZNT) expression.[86,118,119] Finally, it should be pointed out that while FS transitions can be inferred from physical properties other than the viscosity, such as hysteretic behavior in the sample volume as a function of temperature,[147] this should be viewed with caution since those changes could arise from small amounts of crystallization.

The origin of the FS transition remains unclear. In water, it has been ascribed to a competition between two different local structures,[148] as a transition between a high density liquid and a low density one,[149] a merging of relaxation modes[150] and as a crossover from a non-glass forming liquid to a glass forming liquid.[151] In metallic glasses, the FS has been correlated with α and β relaxation times,[152] where the slow β relaxation has an Arrhenius temperature dependence and the primary α relaxation is characterized by a non-Arrhenius behavior. Many structural studies suggest that the FS transition reflects changes in the medium-range order of the liquid and glass.[139] However, combined synchrotron x-ray and quasi-elastic neutron scattering studies find evidence for long-range mass transport, with diffusion lengths of order 100 nm, well beyond the range of the medium range order. This suggests possible chemical phase separation instead of changes in the medium-range order.[97] Clearly, more investigations are needed to clarify the existence of LL phase transitions in metallic liquids, their relation to FS transitions, and the origin of the transitions.

E. Static liquid structure

The results presented in the last section and the MD simulations support the idea of a fundamental connection between local structural excitations and liquid dynamics. However, this is based on a correlation; a causal connection is needed to confirm this. Like the glass transition, this is a central fundamental question that is as yet unanswered. One way to explore it is to examine the connection between various features of the structure and liquid fragility. That, however, first requires a discussion of how the structure of a liquid is described.

The structure of a liquid is typically expressed in terms of the pair distribution function (PDF), $g(r)$,

$$g(r) = \frac{1}{4\pi r^2 n_o N} \sum_{i,j} \langle \delta(r - |r_i - r_j|) \rangle, \tag{8}$$

where r_i is the position of the ith atom at time t, n_o is the atomic density of N atoms, and the brackets, $\langle \ldots \rangle$, indicate a thermal average. This can be calculated directly in molecular dynamics simulations. Experimentally, it is obtained from the Fourier transform of the structure factor, $S(q)$, which is calculated from x-ray, neutron, or electron scattering data. Since liquids and glasses are isotropic, the angular variables of the Fourier transform can be integrated out, giving the following relation between $S(q)$ and $g(r)$:

$$4\pi r^2 n_o N\,(g(r) - 1) = \frac{2}{\pi} \int_0^\infty q(S(q) - 1) \sin(qr)\, dq. \tag{9}$$

To illustrate the quality of scattering data that can be obtained for metallic liquids using levitation techniques and synchrotron x rays, the measured $S(q)$ data for a $Cu_{49}Zr_{45}Al_6$ liquid are shown as a function of temperature in Fig. 6; the corresponding $g(r)$ data are shown in Fig. 7.

As shown, the changes in the structure with temperature are very subtle, yet the corresponding changes in the viscosity are enormous. How such minor changes in the structure can result in large

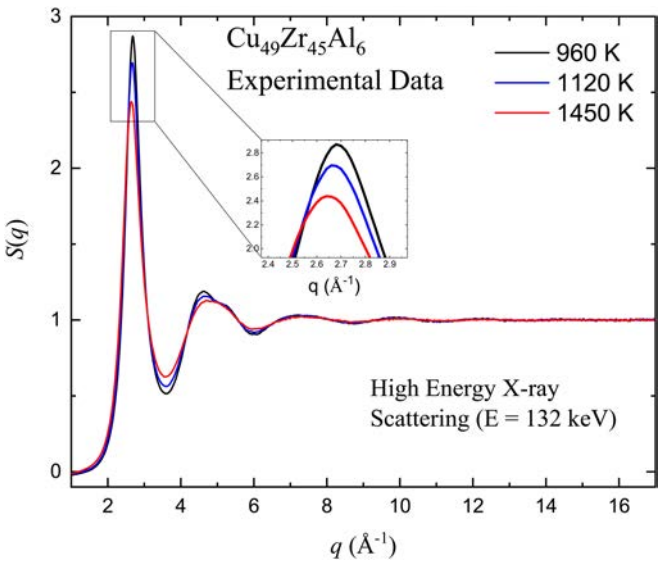

FIG. 6. Measured $S(q)$ for a $Cu_{49}Zr_{45}Al_6$ liquid as a function of temperature. Reproduced from Chen *et al.*, J. Chem. Phys. **155**, 104501 (2021).[153] Copyright 2021 AIP Publishing LLC.

changes in dynamical behavior is a fundamental question that still needs to be addressed.

Another question relates to the thermal expansion of the liquid. For most solids and liquids, the temperature coefficient of volume expansion ($\alpha = (1/V)\,dV/dT$, where V is the volume and T is the temperature) is positive, a result of the anharmonic part of the interatomic potential. The expansion coefficient can be determined directly from the measured volume of the sample, or for crystalline solids, it can be obtained from measured structure factors and pair distribution functions. Shifts in the peaks of the pair correlation function as a function of temperature allow changes in the atomic distances to be determined for different coordination shells, giving the linear expansion coefficient for each shell, β. For isotropic expansion, β is equal to $\alpha/3$. However, measurements in some metallic liquids show an anomalous decrease in the position of the first peak in $g(r)$ with increasing temperature, i.e., $g(r_1)$, suggesting a negative thermal expansion coefficient.[73,154–156] In contrast, measurements of the position of the first peak in the structure factor, $S(q_1)$, as a function of temperature indicate a positive volume expansion in all liquids studied,[74] but the exponent relating the volume to the first peak position ($v \propto (q_1)^{-\varepsilon}$) is 2.28 rather than the expected value of 3 from Ehrenfest's relation.[157] Various explanations for the anomalous expansion coefficient have been offered, including a temperature dependence of the chemical short-range order, leading to a shift in the contribution from partial pair correlation functions[154,158] and decreasing coordination number of the clusters with increasing temperature, forming stronger bonds between atoms and a consequential decrease in the atomic separation.[73] It is important to note, however, that for liquids, a precise definition of the nearest neighbor shell is complicated by contributions to the nearest neighbor shell from overlap of higher order coordination shells. In line with this, more recent constant volume molecular dynamics studies indicate that the apparent shift of the position of the first peak in $g(r)$ can result from the asymmetric shape of the first peak in $g(r)$, with the asymmetry increasing with temperature due to spreading in the distances between neighboring atoms.[159,160] This agrees with results from an analysis of the radial probability density[161] and with a combined molecular dynamics and reverse Monte Carlo study.[162] As discussed in Ref. 160, MD simulations show that the position of the first peak in $g(r)$ is determined from multiple sources: (i) the skewness of the peak, (ii) topological and chemical ordering, and (iii) change in atomic volume with temperature. While it appears that the anomalous expansion coefficient is becoming better understood, further experimental and MD studies would be useful, particularly to see why some metallic liquids show the anomalous behavior while others do not.[73]

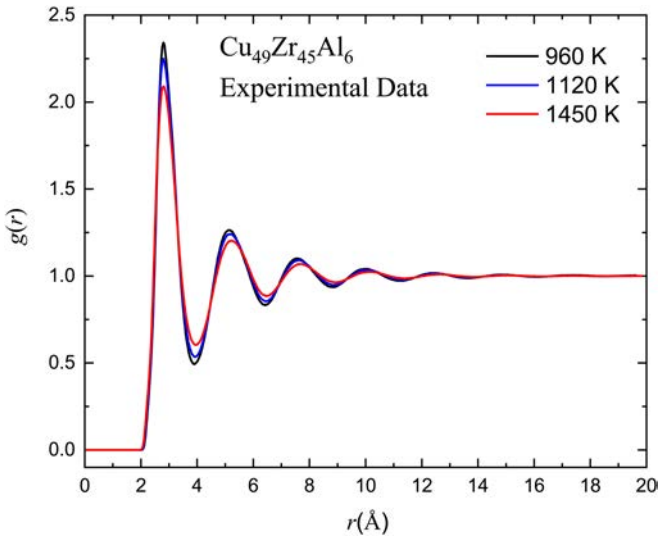

FIG. 7. Measured $g(r)$ for a $Cu_{49}Zr_{45}Al_6$ liquid as a function of temperature. Reproduced from Chen *et al.*, J. Chem. Phys. **155**, 104501 (2021).[153] Copyright 2021 AIP Publishing LLC.

F. Short range structural order and dynamics

The structure factor, $S(q)$, and the pair distribution function, $g(r)$, are one-dimensional representations of a three-dimensional structure. Uniquely identifying actual atom positions from such data is not possible. Techniques such as the Reverse Monte Carlo (RMC) method have been used to find a structure that reproduces the measured $g(r)$ or $S(q)$,[163–168] but it does not produce a unique structure. The structure obtained is the most random one that is consistent with the measured data. Also, the measured $S(q)$ is the result of several partial structure factors (three for a binary alloy, $S(q)_{11}$, $S(q)_{22}$, and $S(q)_{12}$), making interpretation even more difficult. By combining x-ray scattering studies with elastic neutron scattering studies of alloys prepared with different isotopes, it is

possible to determine the partials for binary alloys,[81,169–172] although this becomes increasingly much more difficult for alloys containing more than two elements and is not practical even for ternary liquids.

The structure of the liquid is typically viewed in terms of local ordering units, determined from such an analysis of the measured data for $S(q)$ or $g(r)$. Three methods are most commonly used to describe these local units: (i) the bond-orientational order, (ii) the common neighbor analysis, and (iii) the Voronoi polyhedral analysis. For (i), the bond orientations are expressed in terms of spherical harmonics, $Y_{lm}(\theta,\phi)$, where θ is the polar angle and ϕ is the azimuthal angle, both measured in some specified reference system. The bond-orientational parameter is then calculated by summing over all nearest-neighbor bonds, N_b,

$$\langle q_{lm}\rangle = \frac{1}{N_b}\sum_{j=1}^{N_b} Y_{lm}(r_{ij}). \tag{10}$$

To avoid counting as different structures' equivalent structures that may be oriented differently, the rotational invariant combination is used to give the corrected bond orientational parameter, Q_l,

$$Q_l = \sqrt{\frac{4\pi}{2l+1}\sum_{m=-l}^{l}|\langle q_{lm}\rangle|^2}\,. \tag{11}$$

For the common neighbor analysis, each pair of atoms is taken to be a "root pair" and the local order for this pair is described in terms of four integer indices.[173,174] The first index indicates the peak in $g(r)$ for which the root pair belongs; the second index is the number of atoms that are nearest-neighbors to the root pair; the third index is the number of pairs of nearest-neighbor atoms that are close enough to form a bond; the final index classifies clusters with identical sets of the first three indices but with different bond arrangements. The most used analysis is the Voronoi analysis, in which a line segment is drawn from a central atom to all nearest neighbor atoms and normal planes bisecting these lines are constructed.[175,176] The intersection of these planes gives a three-dimensional polyhedron that is characterized by indices of the form $<n_3,n_4,n_5,n_6,n_7>$, where the subscript indicates the number of edges on the face and n indicates the number of such faces. The results from all three methods describe the liquid structure in terms of short-range ordered (SRO) clusters. Icosahedral ordering is most commonly found, although other types of SRO are also identified. As will be mentioned in Sec. III B, this local ordering is important for nucleation[56,177] and also gives rise to dynamical heterogeneities.[178,179]

A natural question is whether the SRO is linked to fragility. One approach to answering this is to examine the nature of the interatomic potential. It has been argued that glass jamming is associated with a decreased free volume,[180] which would be less for harder atoms (steeper repulsive potentials). This suggests that stronger liquids will have a steeper repulsive component of the interatomic potential, which is in agreement with MD simulations studying the change in harmonicity with changes in the Lennard Jones potential.[181] An experimental examination can be made from the pair correlation function, since the potential of mean force between two atoms, $U_m(r)$, (typically used as a first-approximation to the interaction potential[182]) can be defined in terms of $g(r)$,[183]

$$\frac{U_m(r)}{k_BT} = -\ln[g(r)], \tag{12}$$

where T is the temperature in absolute units. The low-r limit of $g(r)$ can be expressed as[184]

$$g(r) = C(r-\sigma)^{\lambda}, \tag{13}$$

where C is a fitting constant, σ is the average ionic core diameter (calculated from a weighted average of the liquid's constituent elemental ionic core diameters collected from the literature[185]), and λ is the steepness of the effective interaction potential. An examination of experimental scattering data shows that λ decreases with increasing T_A/T (Fig. 8), consistent with a decrease with increasing fragility. It is noteworthy that the cohesive energy also decreases with increasing T_g/T^*, corresponding to an increasing fragility (Fig. 9). The correlations between the strength of the repulsive part of the potential and the cohesive energy with fragility suggest that fragility is related to the interatomic potential. It should be pointed out that studies based on the high frequency shear modulus in metallic glasses reached an opposite conclusion regarding the stiffness of the potential and fragility, finding that a small value of λ correlates with a smaller value of m (i.e., a stronger glass).[184] The reasons for the differences from the two studies of the correlation between fragility and the stiffness of the potential are unclear. The structure of the liquid at high temperature is dominated by short range order,

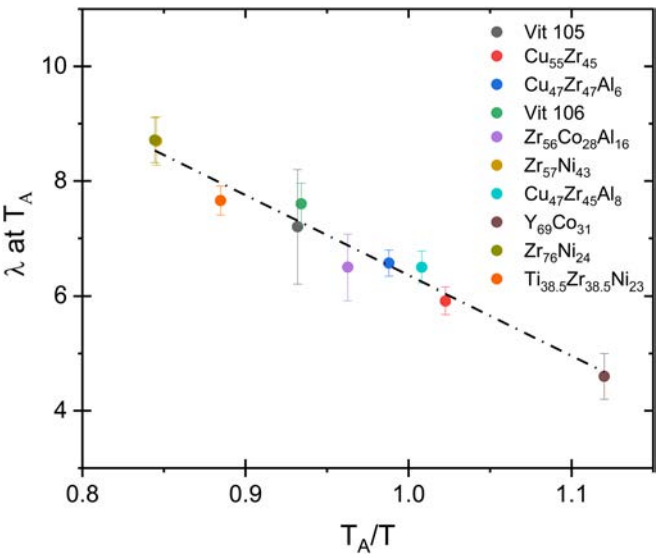

FIG. 8. The steepness of the low-r side of the first peak in $g(r)$ at the temperature T_A, as a function of T_A/T (a measure of the fragility) for several metallic alloy liquids (data taken from Ref. 186).

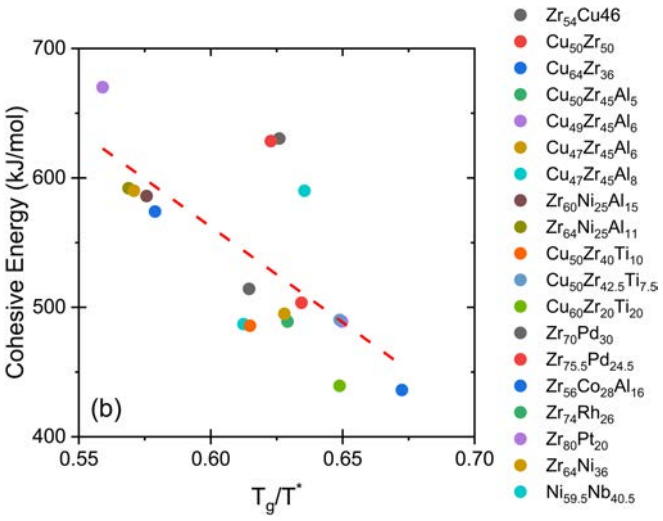

FIG. 9. Cohesive energy as a function of T_g/T^* (a measure of the fragility) for several metallic liquids (data taken from Ref. 111).

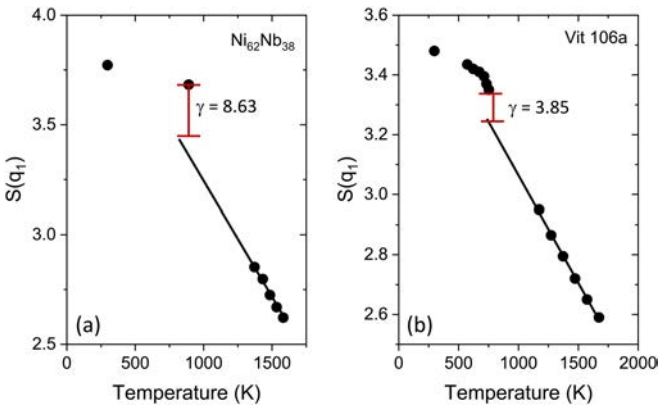

FIG. 10. (a) $S(q_1)$ for $Ni_{62}Nb_{38}$ (a fragile metallic glass) and (b) for Vit 106a ($Zr_{57}Cu_{15.4}Ni_{12.6}Al_{10}Nb_5$), which is a strong glass as a function of temperature (experimental data from Ref. 189).

while as the temperature is decreased below T_A, the structure becomes increasingly dominated by the medium range order. Is it possible that this difference arises because one measurement was made in the supercooled liquid and the other in the glass? Currently, there exist only these two studies; further investigations into reasons for the difference are needed.

G. The importance of medium range order

The discussion in the last section focused on the influence of the interatomic potential and the SRO on properties such as fragility. However, MD calculations indicate that the change in the temperature dependence of the activation energy of the viscosity as the temperature increases below T_A is due to the onset of cooperativity, with interactions extending beyond the nearest neighbors.[116] From these considerations, above T_A, the transverse phonons should be localized since the distance traveled during their lifetime is less than the atomic spacing and there should be no correlations beyond the nearest neighbor atoms. It has been argued that the correlations observed in $g(r)$ beyond the nearest neighbor peak do not reflect correlations among the atoms, but instead represent coarse-grained density correlations that interact via long wavelength longitudinal phonons, which do exist above T_A.[187] These arguments suggest that medium-range order (MRO) may be more relevant than SRO for understanding metallic liquids. While the short range order will be a strong function of the interatomic potential and will, therefore, be highly specific to the elemental composition of the liquid, medium range order will be more general and could lead to similarities observed in many of the properties of metallic liquids.[187]

Experimental scattering studies support this view. The height of the first peak in the measured structure factor, $S(q_1)$, for $Ni_{62}Nb_{38}$ (a fragile metallic glass) is shown as a function of temperature in Fig. 10(a). It is shown for Vit 106a (a strong glass) in Fig. 10(b). As illustrated, an extrapolation of high temperature data (shown by the solid lines) to the values at T_g is different for the two glasses. There is a significant mismatch between the extrapolated data and the data at T_g for the $Ni_{62}Nb_{38}$ liquid, suggesting that rapid ordering must occur upon approaching T_g. The mismatch is much smaller for Vit 106a, suggesting that the liquid is ordering continuously with decreasing temperature toward T_g. From the perspective of heating instead of cooling, the fragile $Ni_{62}Nb_{38}$ liquid quickly loses memory of the more ordered state above T_g, while the strong Vit 106a liquid maintains that memory to higher temperatures. This is an experimental verification of the structural origin of fragility visualized by Angell[91] that was mentioned earlier. It also points to the definition of a structural fragility parameter, γ,

$$\gamma = 100 \left[\frac{S(q_1)_{glass} - S(q_1)_{extrapolated\ liquid}}{S(q_1)_{glass}} \right]_{T_g}. \quad (14)$$

As shown in Fig. 11, γ is strongly correlated with the liquid kinetic fragility, measured here in terms of D^* [Eq. (3)]. Since γ is determined from the first peak in $S(q)$, which is a measure of the order over large distances, this strongly suggests that MRO plays a significant role in the fragility. The importance of MRO is also supported from measurements of $g(r)$.[189] For a variety of supercooled liquids with a range of fragilities, only the fourth peak appeared to correlate with the fragility.

Since the temperature-dependent change of $S(q_1)$ appears to be related to fragility, signaling an importance of MRO, it is useful to examine the quantity $\tilde{S}(q_1, T) \equiv S(q_1, T) - 1$, where q_1 is the location of the first peak. This quantity plays the analog of an order parameter. At infinite temperature, the liquid will be a gas and will have no structural order, i.e., $S(q_1, T) = 1$, so $\tilde{S}(q_1, T) = 0$. Below the crystallization temperature, the liquid will become a crystal and the peak at q_1 will diverge, becoming a Bragg peak, so $\tilde{S}(q_1, T) \to \infty$. Theoretically, $\tilde{S}(q_1, T)$ follows a Curie–Weiss

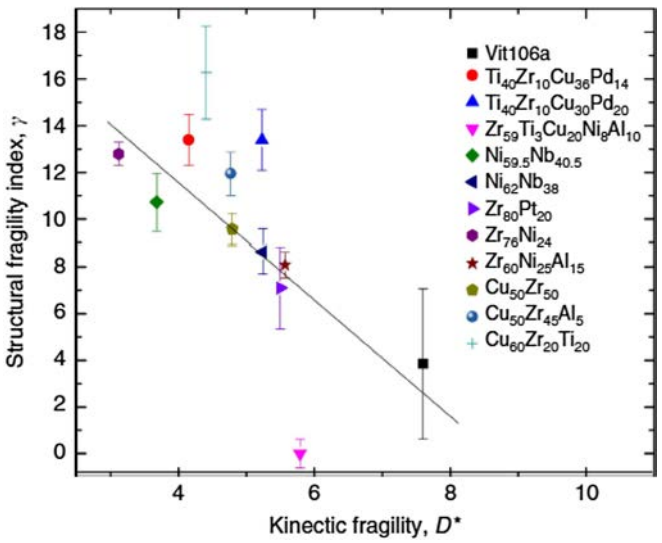

FIG. 11. A correlation between the structural fragility index, γ, and the kinetic fragility index given by D^* for several metallic alloy liquids. Reproduced from Mauro *et al.*, Nat. Commun. **5**, 4616 (2014).[188] Copyright 2014 Springer Nature.

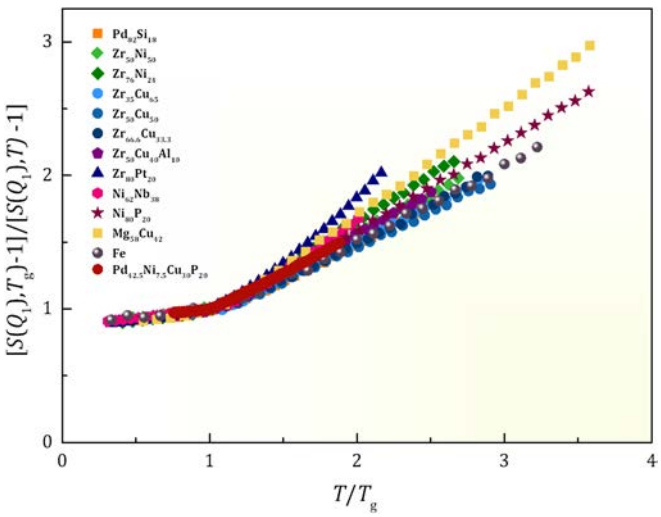

FIG. 12. The quantity $1/(S(q_1, T) - 1)$ normalized to the value at T_g as a function of temperature, showing a Curie–Weiss behavior. Reproduced from Ryu *et al.*, Sci. Rep. **9**, 18579 (2019).[191] Copyright 2019 Author(s), licensed under a Creative Commons Attribution 4.0 License.

law,[190,191]

$$\widetilde{S}(q_1, T) = \frac{C}{T - T_{IG}}, \tag{15}$$

with T_{IG} playing the role of the Curie temperature, T_C. The values of $1/(S(q_1, T) - 1)$, normalized to the values at T_g, are shown as a function of the temperature in Fig. 12. The data deviate from the Curie–Weiss behavior below T_g because the structural changes become kinetically arrested. However, when the high temperature data for the supercooled liquid (i.e., above T_g) are extrapolated they appear to follow a Curie–Weiss behavior, as predicted. In analogy to the divergence in the magnetic susceptibility at T_C due to the onset of long-range magnetic order, the divergence in $\widetilde{S}(q_1, T)$ likely signals the onset of long-range density fluctuation correlations in the liquid.[191] Surprisingly, T_{IG} is negative; this may reflect a pseudo-spin model of local shear fluctuations,[191,192] but further investigation is needed to confirm this. The temperature T_{IG} is also argued to be the point at which an ideal glass stated is reached. It should be pointed out, however, that the values measured for T_{IG} should be viewed with caution; experimental studies show that they depend on the temperature range used for extrapolation.[153] This reflects a nonlinear temperature dependence for $S(q_1)$, which has been widely observed and taken to signal a crossover in dynamical and structural processes. It is also important to note that only one set of experimental data ($Pd_{42.5}Ni_{7.5}Cu_{30}P_{20}$) is shown in Fig. 12. All of the other data were obtained from MD simulations, which can be strongly influenced by the accuracy of the potential used. More experimental data for alloy liquids and a verification of the accuracy of the embedded atom potentials by comparisons with MD predictions and experimental data for dynamical and structural properties (such as in Ref. 153) are needed to verify the correlation.

The rate of change in the first peak height of the supercooled liquid as the temperature approaches T_g correlates with fragility. It also appears that the height of the first peak in the structure factor, $S(q_1)$, may reflect the MRO and correlate with fragility.[193] However, unlike the Curie–Weiss results shown in Fig. 12, which contain only one experimental system, this correlation is based on MD data and experimental data for 10 metallic alloy liquids, including Pd-, Pt-, Zr- Fe-, Ni-, and Mg-based ones. Experimental data also further indicate the importance of the structure factor, showing that glass formability is linked with an increased width of $S(q_1)$.[194]

As discussed, the real space characterization of the liquid is the pair distribution function (PDF), $g(r)$, which is related to the reduced PDF,$G(r) = 4\pi r n_0 [g(r) - 1]$, where n_0 is the number density. The first peak in $G(r)$ represents the nearest-neighbor atoms; it is relatively sharp and has the largest amplitude. Ornstein and Zernike[195] showed that beyond the first peak, $G(r)$ should decay exponentially as

$$G(r) = 4\pi r n_0 [g(r) - 1] \approx G_0(r) \exp(-r/\xi_s). \tag{16}$$

The structural coherence length, ξ_s, gives a measure of the MRO and is a function of the physical density and the strength of nearest neighbor correlations.[187] For temperatures greater than T_A, the phonons are localized and atoms cannot communicate beyond nearest neighbors; the coherence length is then of the order of the nearest neighbor spacing. It is expected to increase with decreasing temperature and is simply related to the temperature-dependent

number of atoms in a coherence volume, n_c,

$$n_c(T) = n_o\,(\xi_s\,(T))^3. \tag{17}$$

Fits of Eq. (16) to experimental data for one metallic glass ($Pd_{42.5}Ni_{7.5}Cu_{30}P_{20}$), MD data for several other metallic glasses, and a number of silicate and other inorganic glasses suggest a correlation between $\xi_s(T_g)/a$ (where a is the average nearest-neighbor distance) and the cube root of the kinetic fragility factor, i.e., $m^{1/3}$.[193] This indicates that there should also be a correlation between n_c and m, with a larger coherence number giving rise to a more fragile liquid.

Based on a Fourier transform of the Ornstein–Zernike equation, the first peak in $S(q)$ for a liquid should be a Lorentzian.[183,187] In this case, the peak amplitude will be high and the coherence volume will be large; if it has a more Gaussian character, the peak height will be lower and the coherence length will be shorter. A more Lorentzian peak is, then, suggested to be evidence for a more ideal glass structure.[187] This result implies that fragility is directly related to the ideality of the structure; the more ideal the glass or liquid the more fragile it is. Studies suggest that ω_L/ω_G [the ratio of the Lorentzian to Gaussian widths in a Voigt fit to the first peak in $S(q)$] is related to $m^{1/3}$.[193]

Collectively, then, fragility is argued to correlate with various aspects of the medium range order, including the rate of change in the first peak of the structure factor ($S(q_1)$) near T_g,[187,188,193] the height and shape of $S(q_1)$,[193] the position of higher order peaks in $g(r)$ and the correlation length of $G(r)$ through the Ornstein Zernike relation.[187,193] However, as for Fig. 12, in most cases, only one experimental dataset exists to check these correlations; all of the other data were generated from MD simulations. Additional experimental data are needed to firmly establish these points. Furthermore, it is natural to ask whether these correlations with fragility are also valid for high temperature liquids. Our initial investigations of a few liquids suggest that the answer might be yes. For example, as mentioned, the MD simulations indicate that at the glass transition temperature, the ratio ω_L/ω_G is proportional to the cube root of fragility, $m^{1/3}$.[193] As shown in Fig. 13, a similar correlation is found in experimental data for a few liquids at T_A, which as mentioned earlier is experimentally related to T_g.[99] It should be pointed out that the values of the widths vary depending on the q-range over which the first peak is fit. The results in Fig. 13 were obtained by fitting between the inflection points of the peak, which were determined from the first derivatives, giving a systematic approach for all the liquids studied. Also, the measurements of fragility at T_g are strongly dependent on the relaxation stage of the glass and the method used to measure the fragility (i.e., either from the slope of the viscosity at T_g or from DSC measurements[196]). Building on earlier discussions and allowing the inclusion of measurements of liquids that do not form glasses, other measures of fragility, such as T_A/T^*, might be considered. Studies in more liquids and glasses as well as an examination of other features of the first peak in $S(q)$ that are argued to correlate with fragility are needed. However, the results shown in Fig. 13 are promising.

All of these data suggest that the dynamics are related to the medium range order, not the short-range order (SRO). However, the discussion in Sec. II F argued for a correlation with the SRO

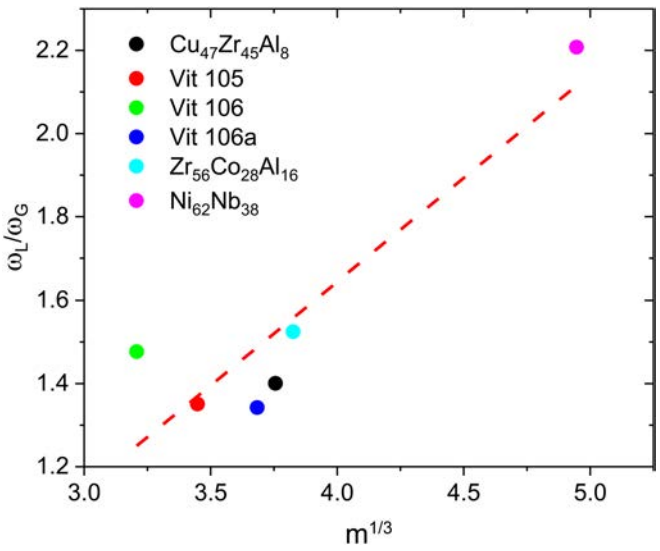

FIG. 13. The correlation between the ratio of the Lorentzian width, ω_L, to the Gaussian width, ω_G from a Voigt fit to the first peak in $S(q)$ for liquid metals at T_A and the cube root of the fragility parameter, m.

through the properties of the interatomic potential. So, which is it? Probably they are both important. For example, recent experimental studies have shown a large fragility in a Mg–Cu–Y glass with composition,[197] supporting the importance for short-range order. Also, while the interatomic potential is clearly most important for SRO, this also influences the MRO, as evident from studies of the Ornstein and Zernike equation.[187] Sorting this out will lead to an improved understanding of how the structure and dynamics are related and perhaps a better informed understanding of fragility.

H. But the liquid structure is not static—The Van Hove function

Since liquids are dynamic, with the atoms moving on picosecond or nanosecond timescales depending on the temperature, $S(q)$ and $g(r)$ give only give a snapshot of the liquid structure. The Van Hove function (VHF) gives a picture of the dynamic structure of the liquid. It is the time-dependent pair correlation function that describes how $g(r)$ decays with time.[198] It is defined as

$$G(r,\,t) = \frac{1}{4\pi r^2\,\rho_o\,N}\sum_{i,j}\left\langle \delta\,(r\,-\,|r_i(0)\,-\,r_j(t)|)\right\rangle, \tag{18}$$

where $r_i(t)$ is the position of the ith atom at time t and <…> denotes a thermal average. Until recently, the VHF was obtained primarily from computer simulations.[199–201] For only a few cases were measurements of $G(r,\,t)$ possible, from inelastic neutron scattering data for metallic liquids at the melting temperature,[202] and from inelastic x-ray scattering studies for water.[203,204] Recent advances in the intensity and energy resolution of neutron scattering sources[205] and the advent of levitation facilities that are

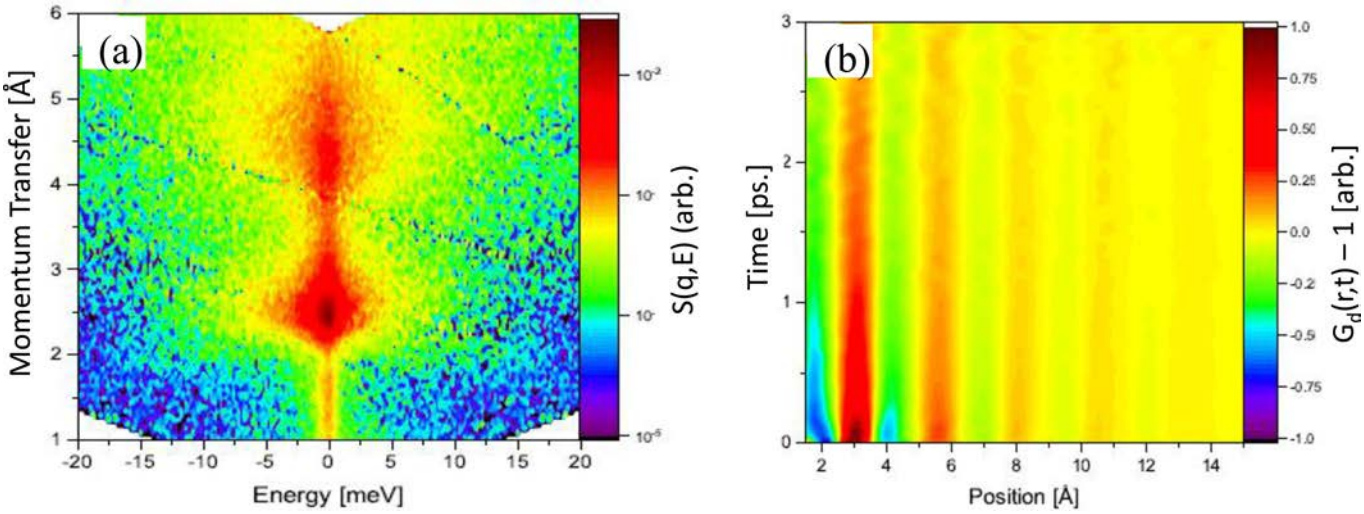

FIG. 14. (a) Measured dynamic structure factor, $S(q,E)$, for $Zr_{80}Pt_{20}$ at a temperature of 1833 K with an incident neutron energy of 20 meV. (b) The distinct part of the Van Hove function, $G_d(r, t) - 1$, at the same temperature. Reproduced from Ashcraft *et al.*, J. Chem. Phys. **152**, 074506 (2020).[84] Copyright 2020 AIP Publishing LLC.

optimized for neutron scattering[77,206] have greatly improved the quality of the data that can be collected, now allowing accurate measurements of $G(r, t)$ to be made over a range of temperatures in equilibrium and supercooled liquids.

Experimentally, $G(r, t)$ is obtained by a double Fourier transform of the dynamical structure factor, $S(q, E)$, which is obtained from inelastic scattering measurements.[84,187] Examples of the measured $S(q, E)$ and $G(r, t)$ from a recent study of liquid $Zr_{80}Pt_{20}$[84] are shown in Fig. 14; the measurement and calculation methods are discussed in that reference. The VHF contains two parts, the self-part, $G_s(r, 0)$, which describes the single particle, and the distinct part, $G_d(r, t)$, which describes collective density fluctuations in the liquid. The intensity of the peaks in $G_d(r, t) - 1$ decrease in intensity with increasing time [Fig. 14(b)]; at time equal to zero, $G_d(r, 0)$ becomes the snapshot of the pair-distribution function, i.e., $g(r)$.

An integration over the intensity of the positive region in the first peak of $G_d(r, t) - 1$ as a function of time gives $N(t)$, which is proportional to the dynamic coordination number and reflects the average decorrelation time for atoms located in the nearest neighbor shell. By fitting this to a stretched exponential in time, a Van Hove relaxation time, τ_{VH}, can be obtained as a function of temperature. This can then be related to τ_{LC}, the fundamental time for local excitations in the liquid[116] (see Ref. 84 for details). Within error, the activation energy for τ_{VH} (and equivalently τ_{LC}) is the same as the activation energy for the measured shear viscosity above T_A, giving the strongest evidence thus far to a link between local excitations in the liquid structure with the dynamics.[84] So far, however, only this one study exists. Measurements of the VHF in other metallic liquids to temperatures below T_A are needed.

This analysis of the Van Hove relaxation time is based on the decay of the first peak in $G_d(r, t) - 1$. Molecular dynamics simulations, however, suggest that the decay time is not the same for all peaks but increases with increasing distance.[207] This could have important consequences on the understanding of collective dynamics, so experimental verification of this is needed.

III. METALLIC GLASS FORMATION AND STABILITY

It is widely believed that any metallic liquid will form a glass if cooled at a sufficiently rapid rate.[23,208] The problem is to determine which liquids will form bulk metallic glasses at moderate cooling rates (i.e., the glass forming ability or GFA). Many schemes have been proposed for identifying these good glass forming alloys (see Table III.5 in Ref. 209, for example). Unfortunately, many of these can only be justified in hindsight once the glasses are found. Considering that glasses are formed when crystallization is ultimately bypassed, one of the first predictive approaches was based on the value of the reduced glass transition temperature, $T_{rg} = T_g/T_\ell$,[23] where T_ℓ is the liquidus temperature. Alloy liquids with the largest values of T_{rg} should be the best candidates for glass formation since the temperature range over which crystallization can occur is least. Since T_g tends to be a rather weak function of alloy composition compared with T_ℓ, eutectics should be favored points in phase diagrams for good glass formation, which is true in some cases. The magnitude of the viscosity at high temperature is larger in stronger liquids than for fragile liquids (see Fig. 1), so from the Stokes–Einstein relation, the diffusion coefficient is smaller in strong liquids, giving lower nucleation and growth rates for crystallization and leading to improved glass formation. While this has also been a useful predictor in some cases, as pointed out earlier, fragile liquids, such as the organic liquids Sorbitol and Salol, can also form glasses.[98] It was also shown recently in metallic glasses that fragility alone does not give a good prediction of glass formability;[97] a better predictor is the combination of T_{rg} and fragility.

While useful, these approaches all depend on knowing properties of the glass, which can only be known after the glass is made. They are only qualitatively useful, then, in guiding searches for new glasses in different alloy liquids. There are some empirical methods based on *a priori* known properties of the alloy elements that have proven useful. Of these, one based on the following three rules is probably the most widely used:[210] (1) production of multicomponent alloys consisting of more than three elements, (2) size mismatches of over 12% among the three primary elements, and (3) negative heats of mixing for three primary elements. The rapid quenching (of order of 10^5 to 10^6 K/s) methods to produce the earliest metallic glasses gave samples that were a few mm wide and a few μm thick, which had limited utility. The application of these rules, however, have led to the discovery of many metallic glasses with large spatial dimensions (bulk metallic glasses), which were produced at lower cooling rates, similar to those used to produce silicate glasses. In spite of this, the discovery of new glasses remains largely empirical and the search for new glasses by preparing a large number of samples containing different elements and having different compositions remains extremely time consuming.

Emerging approaches for identifying good glass formers include computer modeling, machine learning,[29,30] and combinatorial methods.[26,211] While becoming increasingly popular, machine learning approaches should be used with caution. For example, an expansive study using machine learning techniques to predict glass formation based on a combination of alloy and elemental features of glass forming systems[28] was no more accurate than when random unphysical features were used.[31] Furthermore, neither was as predictive as Inoue's[210] three rules physical approach. However, as will be shown in Sec. III A, if machine learning techniques are used to determine the importance of particular and limited physical features in similar systems, they can yield valuable insight.

A. Are there clues for glass formation in the high temperature liquid?

Computer modeling studies have suggested that glass formation is influenced by short- and medium-range order in the liquid. Local icosahedral order has been a particular focus since it is incompatible with crystal order, making nucleation of crystal phases during cooling more difficult. However, recent computer modeling studies suggest that having a particular short-range order in the liquid is not desirable. Even icosahedral order can promote the nucleation of tetrahedral phases or quasicrystals.[56] Instead, glass formation appears to be favored by having regions of different short-range order in the liquid,[212,213] confusing crystallization.[214,215] This is also argued from Monte Carlo fits to the ideal glass structure.[187,191] Experimental support for a diversity of structural units is found in a correlation for GFA with a larger full width at half maximum of the first diffraction peak.[194] These results are consistent with the best BMGs having a large number of elements, which leads to a wider range of local structures.

By analyzing a large database of metallic glasses, Johnson *et al.*[97] proposed an expression for the critical casting thickness (d_{max}) in terms of the reduced glass transition temperature, T_{rg}, and the fragility, m,

$$\log\left(d_{\max}^2\right) = -10.36 + 25.6\,T_{rg} - 0.0481\,m. \tag{19}$$

However, as already mentioned, the need to know T_g in order to predict glass formation requires first making the glass, so this approach is of limited use for identifying new glass forming alloys. A related approach has led to the development of an expression that is based only on liquid data. As discussed, studies of alloy liquids find a strong correlation between T_g/T^* and T_g/T_A (Fig. 5). As shown in Fig. 15, the liquid expansion coefficient, α, also correlates with fragility.

Based on these correlations, an expression that relates T^*, T_A, and α with T_g was obtained by using machine learning methods to fit to 20 different metallic liquids,[32]

$$\frac{T_g}{T^*} = 0.22584 + 1624.3\,\alpha + 0.47324\,\frac{T_g}{T_A}. \tag{20}$$

As shown in Fig. 16, the predicted values for T_g are in excellent agreement with the measured values.

The training data used to develop the expression for T_g were primarily from Zr- and Ti-based metallic glasses. That it predicts T_g for Ni–Nb glasses suggests that the expression may be generally accurate, but this needs to be checked in other alloys.

A similar expression was developed for the predicted critical casting thickness, d_{max}; the results are compared with measured values in Fig. 17. The predictions are in reasonable agreement with experimental data, but there are some notable exceptions. These are interesting since they indicate that the derived expression does not

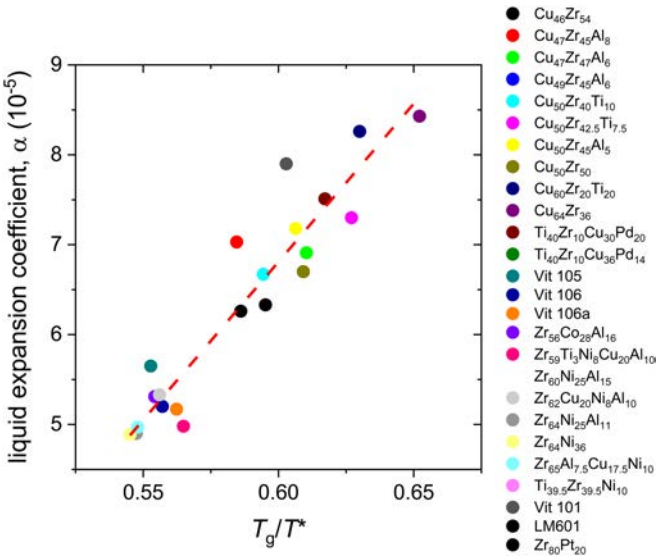

FIG. 15. The correlation of the measured linear expansion coefficient in metallic liquids with the fragility, defined in terms of T_g/T^*. (Data taken from Ref. 32.)

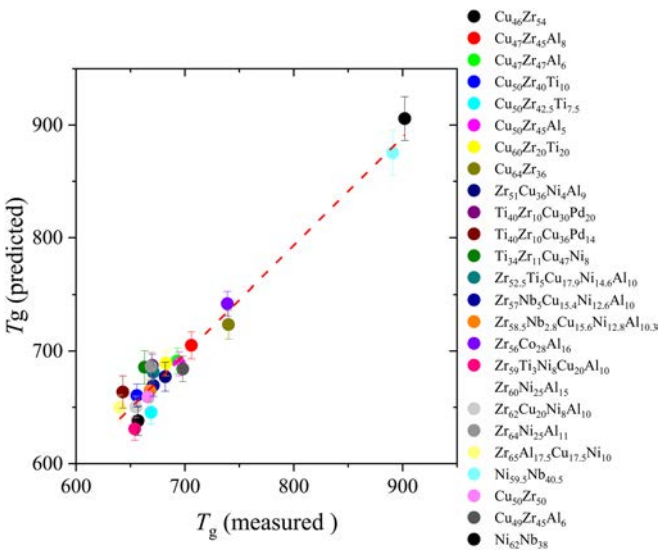

FIG. 16. A comparison between the predicted glass transition temperatures, T_g, and the measured values. (Data taken from Ref. 32.)

take a critical process into account, namely, the crystallization of the liquid. Take the $Pt_{80}Zr_{20}$ liquid as an example. Diffraction studies show the liquid is dominated by icosahedral order, and viscosity measurements indicate that it is a strong liquid. The primary crystallizing phases are β-Zr and Zr_5Pt_3,[216] both of which have a local structure that is very different from the liquid. This difference in local structures should make it difficult to nucleate and grow these phases and thereby make glass formation easier. However, a glass cannot be formed, even with rapid quenching. Instead, the

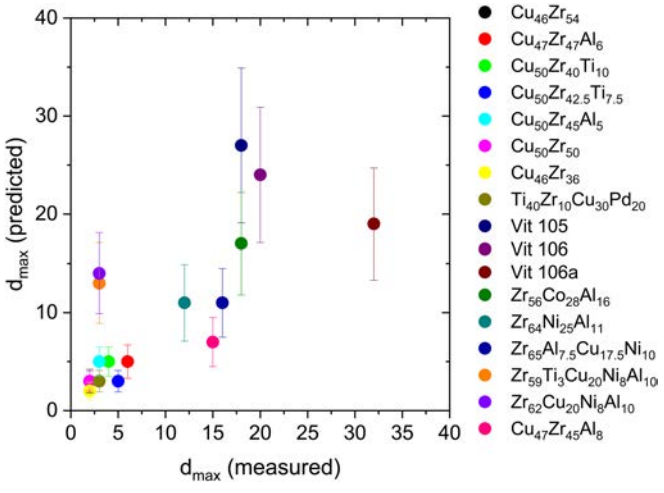

FIG. 17. Predicted critical casting diameter (d_{max}) compared with the measured values. (Data taken from Ref. 33.)

liquid crystallizes to a metastable icosahedral quasicrystal.[217] Similarly, $Cu_{43}Al_{12}Zr_{45}$ is predicted to be a superior glass former to $Cu_{47}Al_8Zr_{45}$, while the opposite is observed experimentally. A diffraction study showed that the primary crystallizing phase for $Cu_{43}Al_{12}Zr_{45}$ is a cubic Laves phase with a large amount of local icosahedral order, causing it to nucleate easily from the supercooled liquid and, thus, decrease glass formability.[33] These are only a few examples that illustrate the importance of understanding crystal nucleation and growth from the liquid. As will be discussed in Sec. III B, ongoing recent work is showing that the classical pictures of nucleation and growth are incorrect and must be modified to develop a quantitative understanding of these processes.

B. Crystallization—New results for nucleation and growth

Glass formation and stability are ultimately limited by crystallization. Crystallization is an activated process that consists of a nucleation step, in which clusters grow and shrink stochastically, and a growth step in which clusters are large enough that shrinking is negligible. While often thought to be two separate processes, within the classical theories of nucleation and growth, growth is simply an extension of the kinetics of nucleation for large clusters.[218]

Focusing first on nucleation, homogenous nucleation occurs randomly in space and time. It is the more relevant type of nucleation for quantitative investigations, but it is uncommon in practice. Heterogeneous nucleation, which occurs at specific sites in the initial phase, is more common, but it is difficult to analyze quantitatively. It depends on the number of heterogeneous sites and their catalytic ability for nucleation, neither of which is generally known. Even though it is less common, studies of homogeneous nucleation are possible under right conditions. The most commonly used model for the analysis of nucleation data is the classical nucleation theory (CNT), which relies on two fundamental assumptions. First, the interface between the nucleating cluster and the original phase is assumed to be sharp and abrupt,[219] and second, each step in the cluster development is assumed to be governed by bimolecular kinetics, with single atoms attaching or detaching from the cluster interface.[220] While these assumptions are reasonable in vapor condensation, for which CNT was originally developed, they are questionable when describing crystal nucleation from a liquid or glass. The structure of the liquid or glass that is adjacent to the nucleus is characterized by short- and medium-range order that may even be similar to that of the nucleating ordered phase, which is not accounted for in CNT.

Nonetheless, since CNT is so widely used, it is useful to briefly discuss the model so that problems can be clearly articulated. The thermodynamic model focuses on the work that is required to form a cluster of the new phase containing n atoms (or molecules), W_n. This is expressed in terms of the negative driving free energy per unit volume, Δg_v, and a positive term associated with the interfacial free energy of the interface between the crystal and the liquid or glass phase, σ. The competition between these two terms leads to a maximum in the work required to create a critical cluster containing n^* atoms or molecules, W_{n^*}. Assuming

that the nucleating cluster is spherical, it is readily shown that[36]

$$W_{n^*} = \frac{16\pi}{3}\frac{\sigma^3}{(\Delta g_v)^2}. \quad (21)$$

A fundamental feature of CNT is that nucleation is a stochastic process, with clusters smaller than n^* biased to shrink while those larger than n^* are biased to grow. To lowest order, then, nucleation is dominated by the rate at which clusters grow larger than n^*. As mentioned, the rate of cluster growth (or shrinking) is governed by the kinetic model for atom attachment to the cluster. For CNT, this is assumed to be dominated by single atoms attaching and detaching (schematically illustrated in Fig. 18). The kinetic steps of attachment and detachment are assumed to involve a movement (often viewed as a diffusive jump) from the liquid onto the crystal interface, and the rates of nucleation and growth are derived from the transition state theory.[221]

With these assumptions, it is straightforward to show that the CNT steady-state nucleation rate is

$$I^s = A^* \exp\left(-\frac{W_{n^*}}{k_B T}\right), \quad (22)$$

where A^* is a dynamical pre-factor that is proportional to Avogadro's number (if the nucleation rate is measured per mole) and the diffusion coefficient in the liquid phase; it is inversely proportional to the square of the jump distance. For an as-quenched glass, CNT predicts that the nucleation rate will be time dependent before it settles into a steady state rate. While this is very important for the crystallization of silicate glasses, it is generally not important for metallic glasses, but it can become evident for crystallization during rapid heating and has been directly measured during the crystallization of a few bulk metallic glasses.[71] It is not typically measurable in supercooled metallic liquids because the kinetics are so fast at high temperatures that steady-state is achieved quickly. (An in-depth discussion of CNT and steady-state and time-dependent nucleation can be found in Ref. 36.)

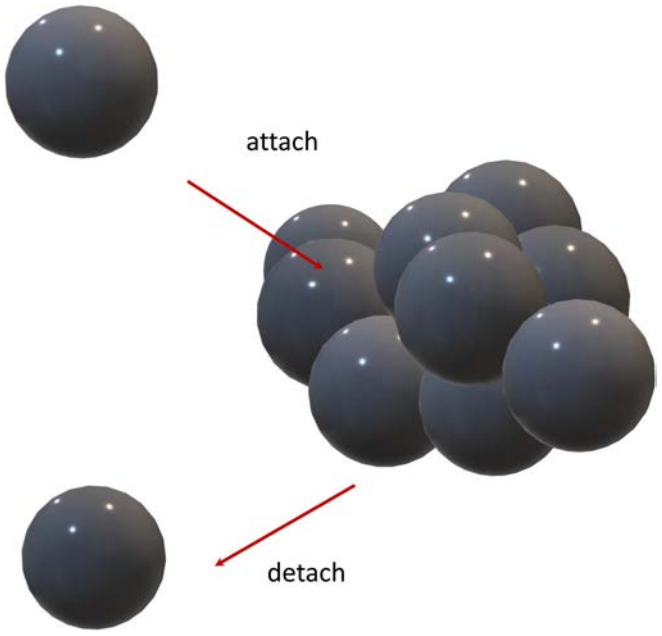

FIG. 18. Schematic illustration of the stochastic attachment and detachment of single atoms or molecules (spheres) for a nucleating cluster.

While the CNT has successfully been used to fit nucleation data in liquids and glasses, there are several problems with the theory. First, the nucleation rate is extremely sensitive to the interfacial free energy ($\sim\exp(\sigma^3)$), which cannot be measured independently, so it becomes a fitting parameter. Second, the order in metallic liquids or glasses next to the nucleating cluster brings into question the sharpness of the interface. As illustrated by MD simulations,[222] small nucleating clusters are neither spherical nor compact, although they become more so as they grow to larger sizes. This is consistent with a wide range of computer simulations, density functional calculations, and experimental studies of nucleation in colloids (see chapter 4 in Ref. 36 for more discussion on this point). This incorrect assumption can cause W_{n^*} (and hence n^*) to be very different from predictions of CNT.[223] A phenomenological model, the diffuse interface model, was developed to address this.[224–226] It has shown some success, particularly in predicting the experimentally inferred positive temperature dependence for σ.[224]

The CNT also fails to consider possible effects of short and medium-range ordering in the liquid, which, as mentioned earlier, can determine the nucleating phase. Icosahedral short range order has been viewed as particularly important.[66] For example, experimental studies of nucleation in $Ti_{39.5}Zr_{39.5}Ni_{21}$ of a metastable quasicrystal phase rather than a stable C14 laves phase indicate that the icosahedral ordering in the liquid lowers the nucleation barrier for the quasicrystal.[56] This also suggests that nucleation is a two-step process, proceeding first by local ordering in the liquid followed by densification during nucleation. Such coupled order parameter processes can also occur between phase transitions, such as the relation between magnetic ordering and nucleation, and a proposed chemical ordering/nucleation process,[227,228] which has been observed in MD studies.[229] Recent studies have gone even further, supporting the idea that in many cases nucleation can have even more than two steps.[230] Such questions are under intense study. How wide an impact multistep processes have on nucleation in supercooled liquids and glasses remains to be seen. In addition to their role in changing the thermodynamics of nucleation, fluctuations in the local structures in the liquid can also lead to dynamical heterogeneities that influence the kinetics of nucleation. Based on MD studies, regions of icosahedral order are slow dynamical regions. A recent MD study showed that these are the regions where nucleation occurs, even to crystal phases with a non-icosahedral structure.[231]

Classical theories of nucleation and growth are based on the transition state theory, which was first developed to calculate the rates of chemical reactions.[221,232] They assume that atoms independently join and leave the nucleating or growing cluster with a frequency, ν, that is determined from the diffusion coefficient in the liquid, D, i.e., $\nu = 6D/\lambda^2$, where λ is a jump distance that is of order

the interatomic spacing. This jump frequency is biased by a thermodynamic term of the form $\exp(-\Delta g^*/k_B T)$, where Δg^* is the free energy difference between the initial state and an activated (or transition) state. However, recent MD studies raise questions about the validity of this kinetic model.[233,234] For illustration, some MD results for nucleation in a Ni–Zr–Al liquid are shown in Fig. 19, with a bcc crystal to the right of an interface (indicated by the red arrow) and the liquid to the left of the interface. These results demonstrate that the densities of the liquid and crystal are very similar, a point that agrees with experimental measurements. There is not enough room for an atom to make a diffusive jump from the liquid to join the interface of the nucleating cluster. So, it must be joined by some other mechanism. Molecular dynamics simulations show that the liquid atoms are joined to the cluster by small changes in their orientational order, adjusting their order parameter to match that of the crystal phase.[234]

In a recent series of publications,[236,237] the problem of growth is reformulated, assuming that interfacial attachment is due to the cooperative structural organization of several atoms on passing through a transition zone (TZ) between short and long-range order as they join the cluster, without the need for diffusive type jumps. Similar to the arguments made earlier for the role of cooperativity in liquid dynamics, they assume that the coherence length for this cooperativity increases with decreasing temperature. Accounting for the cooperativity and assuming that the appropriate lattice vibration modes are those that lead to the formation of the crystal mode (multiplied by a characteristic wavelength of vibration, λ^*, which corresponds to the first Brillouin zone of the allowed lattice vibration), they obtain a new, non-classical, expression for the growth velocity,

$$v_{TZ} = \lambda^* \frac{k_B T}{h} \exp\left(-\frac{\Delta h^\dagger_{AG} - T\Delta s^\dagger_{AG}}{k_B T}\right). \tag{23}$$

Here, $\Delta h^\dagger_{AG}$ is the activation enthalpy; using the Adam–Gibbs relation[104] to include the cooperativity,

$$\Delta h^\dagger_{AG} = \Delta h^* \left(\frac{T}{T - T_K}\right), \tag{24}$$

where Δh^* is the enthalpy for the bond changes with reordering, which must be scaled to the size of the cooperative region, and T_K is the Kauzmann temperature.[238] The activation entropy is

$$\Delta s^\dagger_{AG} = \Delta s^* \left(\frac{T - T_K}{T_\ell - T}\right)^z, \tag{25}$$

where Δs^* is some inherent entropic activation parameter and T_ℓ is the liquidus (or melting) temperature. The exponent, z, is asserted to be related to the ratio of configurations of the growth units in the TZ and the supercooled liquid phases, making it correlated with $-k_B/\Delta s^*$.

Since the Brillouin zone and the liquidus temperatures can be independently measured, this expression for the growth rate has three fitting parameters (provided T_K has been separately measured), which is one more than for the classical expression for the growth rate. It was found to give an improved fit over that of the classical theory to the measured crystal growth rate for a number of silicate and organic liquids,[237] although the additional fitting parameter could explain this improvement.

This approach is clearly more in line with physical interfacial processes between a liquid or glass and the crystal than are the classical theories of growth. Molecular dynamics studies show that many of the assumptions made for interfacial attachment in this model are correct. The spatial movements for incorporation into the crystal interface are small; incorporation is instead dominated by changes in the crystal order parameter for atoms located near the interface. It appears that atoms do attach cooperatively,[233,234] with the number of atoms in the coherence region increasing with decreasing temperature.[234] While there are now two independent MD studies that show this, studies in more systems are needed to confirm that these are general trends. Furthermore, there is no modified analytical model for nucleation that takes these points into account. Clearly, there are a wide range of computer modeling and experimental and theoretical studies that are needed on these issues. Also, while the new expressions appear to give a better fit to crystal growth data, there have been no studies for metallic alloy liquids. Whether the modified kinetics significantly influence physical nucleation and growth processes should be investigated.

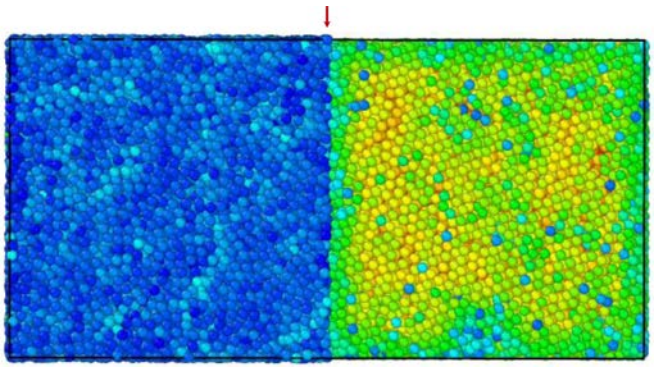

FIG. 19. Molecular dynamics generated crystal/liquid interface for a Ni–Zr–Al liquid. The interface between the liquid (left) and the crystal (right) is indicated by a red arrow (from Ref. 235).

C. Ultrastable glasses and rejuvenation—Opposite sides of the coin

Glass stability, as well as glass formability, is a principal factor for many applications. Pharmaceutical drugs, for example, are often amorphous since they are more readily absorbed in the body; they become less effective when the drugs crystallize as a consequence of aging during storage.[239] The quality of foods such as chocolate and ice cream are also degraded by crystallization (see chapter 17 in Ref. 36), and it is detrimental in amorphous optical materials.[240] Controlled crystallization, however, can also be used to improve the properties of glasses, such as increased

toughness in partially crystallized silicate and metallic glasses (glass ceramics).[11–13] Attaining that control is improved by the advances in the understanding of nucleation and growth discussed in the last section.

Some glasses such as natural amber are extremely resistant to crystallization, maintaining the amorphous structure for millions of years.[241,242] Metallic glasses, however, tend to be metastable, with some crystallizing after only a few hours of aging at room temperature.[243] It was first reported in 2007 that organic dense glasses with exceptional thermodynamic and kinetic stability can be obtained by vapor deposition onto a substrate at a temperature near T_g.[244] These ultrastable glasses have a substantially higher glass temperature (measured on heating the glass) and a lower fictive temperature, T_f, (the temperature at which the glass would be in equilibrium)[245] than those produced by standard methods. A larger surface diffusion with a smaller temperature dependence than the volume diffusion coefficient is believed to play a significant role in forming these deposited glasses. The enhanced surface diffusion allows the atoms to reorganize and find low energy configurations. These glasses typically have a lower enthalpy than glasses prepared by cooling the liquid (thermodynamic stability) and are more resistant to structural changes and crystallization[246] (kinetic stability). Recent reviews of ultrastable vapor deposited glasses can be found elsewhere.[247,248]

Ultrastable metallic glasses have also been produced by deposition on substrates that are near T_g, similar to the conditions for organic ultrastable glasses. Interestingly, the ultrastable $Zr_{65}Cu_{27.5}Al_{7.5}$ metallic glass was kinetically stable, but the enthalpy was larger than the glass prepared by cooling the liquid.[249] This should be investigated in other metallic glasses since it could indicate that thermodynamic and kinetic stability do not necessarily go hand-in-hand. The measured surface diffusion coefficients for a $Pd_{40}Cu_{30}Ni_{10}P_{20}$ were very high,[250] suggesting that the mechanism for producing ultrastable metallic glasses is the same as for the organic glasses. All of these glasses were prepared with the substrate temperature of order 0.7 T_g. While ultrastable metallic glasses have extraordinary hardness (see Ref. 251 for example) and corrosion resistance, which can be used for superior coatings, these substrate temperatures are quite high. This makes the avoidance of oxidation and contamination during deposition difficult, limiting the materials that can be made and, thus, limiting applications. Recently, it was demonstrated that some Zr-based ultrastable metallic glasses can be deposited on substrates that are held at low temperatures (≈0.4 T_g, near room temperature) by decreasing the deposition rate to approximately 1 nm/min.[252] Like those glasses that are deposited at elevated temperatures, these ultrastable metallic glasses show a substantial increase in T_g, (by approximately 60 K in this case) are strongly resistant to crystallization, and have a more homogenous structure. The ability to deposit them at low temperatures greatly increases the substrates that can be chosen, matching them to the desired application. Because of the very low deposition rates used, however, care should be taken to ensure that contamination of the glasses by oxygen or from the ion beam used for the deposition does not occur.

But can macroscopic ultrastable glasses be made? It is possible that metallic glasses could be aged into more stable amorphous states if crystallization could be avoided, but if so like the amber glass this would require an extremely long time for the system to settle into the low energy states in the energy landscape. Investigations of a broad range of Al-based, Mg-based, Cu-based, Ni-based, Ti-based, and Zr-based metallic glasses that had been stored at room temperature for at least 15 years showed that the increased stability was minimal with virtually no statistically significant change in T_g from the as-prepared glasses.[253] This could indicate that a much longer aging time is required, but since some of the aged metallic glasses already showed signs of oxidation and partial crystallization, this is impractical. It may also be that higher temperatures are required since room temperature is significantly lower than the values of T_g in these glasses. Supporting this, room temperature aging studies for 17.7 years in a $Ce_{70}Al_{10}Cu_{20}$ metallic glass, for which T_g is 353 K, were successful in producing an ultrastable glass.[254] These aging studies were made at ∼0.85 T_g, suggesting that higher temperature aging treatments in other metallic glasses could significantly increase the stability. However, while of basic interest, the practical use of this approach remains questionable due to the long aging times. An approach that has been moderately successful is to age under high pressure.[255] An aging treatment of a Pd-based metallic glass for 1 h under 10 GPa increased T_g by 6 K; under 17 GPa, T_g increased by 11 K. The crystallization temperature also increased with increasing pressure. Both results are consistent with an increased stability of the glass; however, the increase in T_g is only 10%–20% of that found in the deposited glasses, indicating that the increase in stability is modest.

A recent novel approach is based on the phenomenon of a reentrant glass transition, in which a glass (glass 1) transforms into a supercooled liquid when heated above its glass transition temperature, T_{g1}, and then forms a second, more stable, glass (glass 2) upon cooling, which has a different glass transition temperature, T_{g2}. This method depends on the existence of a liquid/liquid phase transition in the supercooled liquid, similar to the ones discussed in Sec. II D. A reentrant glass transition has been observed in a variety of glass forming systems, including colloids,[256] spin glasses,[257] molecular glasses,[258] and metallic glasses.[259] To investigate whether this might provide a route to ultrastable glasses, an as-quenched $Pd_{42.5}Ni_{42.5}P_{15}$ metallic glass was heated above T_g under ambient pressure, where it transformed into a second glass, showing an exothermic peak, a decrease in volume, electrical resistivity, and specific heat and an increase in the hardness and Young's modulus.[260] All of these changes are consistent with the formation of a more stable glass. The T_g of the transformed glass is nearly 50 K higher than for the as-quenched glass. These changes in the enthalpy and T_g are comparable to those for ultrastable glasses produced by vapor deposition.

What is the nature of the phase transition from glass 1 to glass 2 in $Pd_{42.5}Ni_{42.5}P_{15}$? This was investigated in a study by Du *et al.*[260] Small angle x-ray scattering and atom probe tomography studies show no evidence for phase separation or chemical segregation. During the transition, the width of the first peak in $S(q)$, obtained from synchrotron studies, decreases sharply on approaching T_{g2}, from 0.43 $Å^{-1}$ for glass 1 to 0.27 $Å^{-1}$ for glass 2, indicating increased medium range structural order. This is much larger than observed during structural relaxation, consistent with the formation of a new, more stable, glass phase. Changes in $G(r)$ are consistent with these results, showing similar short-range order in the two glasses, but with significant changes beyond 6 Å. Reverse Monte

Carlo (RMC) fits to the $S(q)$ data, constrained by EXAFS data for Ni and Pd K-edges, suggest that the structural ordering accompanies the redistribution of P atoms to form more solute-centered local environments, with local clusters that are similar to those in Ni_2P and Ni_3P crystal phases. The size of these clusters also increases, consistent with the increased medium range order.

The change in the glass transition for the ultrastable glass normalized to the glass transition temperature of the metastable one, $\delta T_g/T_g$, appears to correlate with fragility.[249] Since differences between as-quenched glasses and ultrastable ones appear primarily in the medium range order, this is consistent with suggestions made earlier that MRO is correlated with fragility. However, most of the data regarding this correlation are from thin film deposited organic liquids. One deposited glass ($Zr_{65}Cu_{27.5}Al_{7.5}$) was in line with these, showing $\delta T_g/T_g \cong 0.015$ with a fragility of $m \cong 40$ (Fig. 4 in Ref. 249). However, the more recent results for the $Pd_{42.5}Ni_{42.5}P_{15}$ glass, which also has a fragility value of $m \cong 41$,[261] gives a much larger normalized change in the glass transition temperature, $\delta T_g/T_g \cong 0.09$.[260] This ultrastable glass was produced using a reentrant glass transition, possibly explaining the difference with the deposited glass. Yet, a deposited $Zr_{46}Cu_{46}Al_8$ glass ($m \cong 53$) also gave a larger normalized change, $\delta T_g/T_g \cong 0.085$,[252] although this glass was deposited at much lower temperatures relative to T_g than most ultrastable glasses. More work is needed to understand the influence of substrate temperature on deposited glasses, the mechanism for ultrastability when there are reentrant glass transitions, and whether a clear correlation between $\delta T_g/T_g$ and fragility exists.

There are many positive aspects of glass aging; the stability of the glass to crystallization is increased, it becomes harder and more corrosion resistant, and the yield stress is increased. However, aging also leads to embrittlement.[262] This can be improved by a process of rejuvenation, a disordering process that puts the metallic glass into a higher energy state and results in better plasticity.[263–265] In a Zr–Cu–Ni–Al–Nb glass, the fracture toughness and impact toughness nearly doubled with rejuvenation[266,267] and the toughness increased by more than five times.[267] Several approaches have been used for rejuvenation, including cold rolling,[268] shot peening,[269] irradiation,[270] and cryogenic thermal cycling.[263] Cycling between room temperature and cryogenic temperatures has several advantages over the other methods. It is nondestructive and can be applied to macroscopic glasses with large cross sections. Liquids and glasses are characterized by structural and dynamical heterogeneities. The heterogeneous thermal expansion coefficients induce local stresses during cryogenic cycling, leading to glass rejuvenation.[271] By a suitable combination of stabilization and rejuvenation treatments, it may be possible to access structural states for metallic glasses that cannot be reached in other ways,[272] providing a new way to tune glass microstructures for particular applications. Unfortunately, a recent study of BMGs based on Pd, Pt, Ti, and Zr found that rejuvenation by thermal cycling is impermanent, decaying after only one week at room temperature.[273] This has significant implications for the interpretation of previously reported results and indicates the need for characterization standards for new results. There are also profound implications for the use of cryogenic cycling to produce desired properties for applications of metallic glasses.

There are many aspects of rejuvenation that are not well understood. Studies in a $Zr_{46}Cu_{38}Al_8Ag_8$ glass, for example, showed that samples that are well relaxed after annealing for long times are essentially unaffected by cryogenic cycling, while glasses that were aged for a brief time showed a large rejuvenation effect. Interestingly, glasses that were given an intermediate aging treatment showed the greatest rejuvenation effect.[274] The amount of rejuvenation depends on the method of metallic glass preparation; one study showed that it was greater for melt-spun ribbons than for bulk metallic glasses.[263] Also, it appears to work in some metallic glasses and not for others. For example, it was negligible in Ti-based glasses.[275] Using the change in maximum plastic strain, ε_{max}, as a measure of rejuvenation, essentially no change was observed in $Zr_{60}Cu_{20}Co_{10}Al_{10}$ glasses with cryogenic cycling, while a large increase in ε_{max} was observed in a $Zr_{60}Cu_{20}Fe_{10}Al_{10}$ glass.[271] However, the increase in ε_{max} in this glass did not continue with an increasing number of cryogenic cycles; it went through a maximum after about 10 cycles and then decreased with further cycling. This behavior is commonly observed,[273,276] pointing to competing processes. Disorder increases with rejuvenation, but it also increases the atomic mobility, which causes the structural relaxation to a more ordered glass to proceed more quickly. All of these glasses contained a pair of elements with a positive heat of mixing (Cu–Fe, Cu–Co, and Cu–Ni), although the magnitudes are different (greatest for Cu–Fe and least for Cu–Ni). These results indicate that the chemistry can influence the plasticity of the glasses and hence the degree of heterogeneity and the effectiveness of the cryogenic cycling for rejuvenation. In agreement, a recent study of different bulk metallic glasses found that for some BMGs, thermal cycling resulted in a less dense structure with an increase in fracture toughness, while for others, thermal cycling relaxed the glass to a denser structure with a decreased fracture toughness.[276] Chemistry can also influence relaxation processes in the glasses, in particular, the β relaxation,[277] which is correlated with plasticity.[278] Possibly explaining the influence of alloy chemistry on rejuvenation, β relaxation is more pronounced in glasses with stronger elemental bonding.[279]

There have been a few studies of structural changes with the associated changes in dynamics in the glass with cryogenic rejuvenation; these have produced varied results. They consistently show that the location of the first peak in $S(q)$ decreases with rejuvenation, consistent with a decreasing density and disordering of the short-range order.[274] Similar results are obtained in glasses that have been rejuvenated by mechanical deformation.[280,281] A decreasing density is also inferred from HRTEM measurements of $G(r)$, showing a shift in peak positions toward larger values of r.[271] However, one synchrotron x-ray study shows a sharpening of the first peak in $S(q)$, which suggests ordering, not disordering, as would be expected.[282] This study also concluded that atomic re-arrangements in the second neighbor shell contribute more to the relaxation enthalpy than the nearest neighbor shell, in apparent conflict with the results of the study by Kang *et al.*[274] As mentioned, metallic glasses are characterized by structural heterogeneities, which are the source of rejuvenation by cryogenic cycling. Results from x-ray photon correlation spectroscopy measurements indicate that cycling reduces these heterogeneities, homogenizing the relaxation time distribution.[283]

It is appropriate to end this section with a few questions. First, regarding ultrastable glasses, so far a reentrant glass transition has been observed only in one glass system ($Pd_{42.5}Ni_{42.5}P_{15}$). A key question, then, is how common is it? Does it occur only in glasses with a significant covalency in their bonding character, such as metal/metalloid glasses? If it were a phenomenon that occurred in a wider range of metallic glasses, it could provide a practical method for stabilizing bulk metallic glasses for an increased range of applications. Second, the formation of ultrastable glasses and rejuvenation are the result of different, likely competing, relaxation times. While attention is generally focused on α and β relaxation times, it is most likely that the spectrum of relaxation times is larger. More studies are needed to better understand the reasons for rejuvenation and ultrastability and to be able to control these processes to better tailor metallic glasses to specific application. A reoccurring theme in this article is the use of molecular dynamics to give microscopic pictures for dynamical and structural properties of liquids and glasses and to inspire experimental investigations. Some MD studies of rejuvenation have been made and are providing useful information (see Ref. 284 for example). However, many questions remain for further MD investigations, including a demonstration of the assumption of local structural heterogeneities in the thermal expansion coefficients of the metallic glasses, which is the key for understanding cryogenic rejuvenation.

IV. CONCLUSIONS

This Perspective has focused on a few points about metallic liquids and glasses: the connection between the structure and dynamics in supercooled metallic liquids, how these processes may help to identify potential glass forming systems, advances in the understanding of crystallization, which is important for glass formation, and manipulations of the stability of glasses. It must be pointed out that a comprehensive review of any of these topics would be an enormous task and was not attempted here. Also, not discussed were topics such as the origin and nature of glass transition, the physical properties of metallic glasses, particularly mechanical properties, and how these are exploited for practical applications. Finally, while predictors of glass formation in terms of the properties of high temperature liquids and the fundamentals of nucleation and growth were focus topics, other issues such as the considerable influence of micro-additions on glass formation in some cases were not discussed.

The primary focus of this Perspective was to identify themes in current research and raise some questions that point toward further study. Many of these have been mentioned in the text. In metallic liquids, these questions include:

- Is there a fundamental connection between the liquid structure and dynamics, and if so, what is the most appropriate feature of the structure of supercooled metallic liquids that connects them? Is it short range order or medium range order; or is it a competition between the two?
- Liquid/liquid phase transitions have been widely reported in supercooled metallic liquids. Do they actually exist, or are they simply crossover phenomenon? Are they connected to fragility transitions, where a high temperature fragile liquid transforms to a strong liquid at lower temperatures? What is the underlying microscopic mechanism for this transition?
- Molecular dynamics simulations have identified a temperature, T_A, where local structural excitations become cooperative and have a profound influence on liquid dynamics. By scaling the temperature to T_A and the viscosity to the extrapolated value at infinite temperature, η_o, a universal curve was identified. Related to this, but not discussed here, is the identification of a minimum viscosity in metallic liquids that is related to quantum mechanics.[285] Both the universal curve and viscosity minimum are of interest in fields far beyond metallic glasses, including quark-gluon plasmas and Bose–Einstein condensates.
- The electrical resistivity changes abruptly at T_A, which provides strong evidence for a structural origin of the dynamic crossover, in agreement with molecular dynamics studies. However, most surprising is that the temperature dependence of the resistivity vanishes above this temperature. This is not predicted by any existing theory of the electrical resistivity of metallic liquids and points to the need for new theoretical models.
- Not discussed is that the Stokes–Einstein relation, which connects the viscosity and the diffusion in the liquid, is known to fail as the liquid is cooled, but where does that occur? Is it at the mode-coupling temperature or at the higher temperature, T_A, where the dynamics become cooperative? Both temperatures have been suggested.

Several themes and questions regarding glass formation were also discussed.

- The properties of the high-temperature liquid were shown to be a good predictor of glass transition, but less so of glass formability. This needs to be investigated for a wider range of glasses, however.
- Failures to predict glass formation were shown to hinge on questions of crystallization, involving nucleation and growth. Relevant to this, nucleation and growth were shown to be more complicated than typically viewed. Molecular dynamics studies showed that instead of diffusive motions for liquid atoms to join crystal clusters, this involves a change in their local order parameter with very little physical movement. Furthermore, instead of joining individually, atoms join cooperatively. Neither of these features is incorporated in the classical theories of nucleation and growth, pointing to the need for an additional study.
- There is a great deal of activity in producing ultrastable and rejuvenated glasses, which has significant importance for applications. The mechanisms for these processes, however, are still poorly understood, pointing to the need for further research. There has been a good deal of interest in the perfect glass, which has long range density correlations but no positional order.[187] It may be that the ultrastable glasses are a physical manifestation of this,[286] which bears further investigation.

Future work should address these questions with experimental studies. Additionally, a growing theme, which was discussed several times in this Perspective, is the power of computer simulations. These can guide experimental investigations and greatly assist interpretations of data. Additionally, combinatorial approaches, machine learning, and artificial intelligence have an enormous

potential to probe more deeply. The future will undoubtably see an expanding scope for these techniques. Because they are atomic systems and lack directional bonding metallic liquids and glasses are among the simplest amorphous systems. They are, therefore, ideal for delving into questions of the glass transition, fragility, and the relations between the structure and dynamics in complex systems. Metallic glasses are also poised to become important technological materials. These systems, then, offer opportunities for many future fundamental and practical investigations.

ACKNOWLEDGMENTS

This work was partially supported by the National Science Foundation (NSF) under Grant No. DMR-19-04281 and by NASA under Grant No. NNX16AB52G. Any opinions, findings, and conclusions or recommendations expressed in this material are those of the author and do not necessarily reflect the views of the National Science Foundation nor of NASA. Thanks are given to Fangzheng Chen, Anup Gangopadhyay, A. L. Greer, and Zohar Nussinov for useful discussions.

AUTHOR DECLARATIONS

Conflict of Interest

The authors have no conflicts to disclose.

Author Contributions

K. F. Kelton: Conceptualization (equal); Formal analysis (equal); Investigation (equal); Writing – original draft (equal); Writing – review & editing (equal).

DATA AVAILABILITY

The data that support the findings of this study are available from the corresponding author upon reasonable request.

REFERENCES

[1]H. W. Ng, R. Hasegawa, A. C. Lee, and L. A. Lowdermilk, Proc. IEEE **79**(11), 1608–1623 (1991).
[2]P. H. Tsai, Y. Z. Lin, J. B. Li, S. R. Jian, J. S. C. Jang, C. Li, J. P. Chu, and J. C. Huang, Intermetallics **31**, 127–131 (2012).
[3]J. P. Chu, J. S. C. Jang, J. C. Huang, H. S. Chou, Y. Yang, J. C. Ye, Y. C. Wang, J. W. Lee, F. X. Liu, P. K. Liaw, Y. C. Chen, C. M. Lee, C. L. Li, and C. Rullyani, Thin Solid Films **520**, 5097–5122 (2012).
[4]J. Schroers, G. Kumar, T. M. Hodges, S. Chan, and T. R. Kyriakides, JOM J. Miner. Met. Mater. Soc. **61**(9), 21–29 (2009).
[5]V. Wessels, G. Le Mene, S. F. Fischerauer, T. Kraus, A. M. Weinberg, P. J. Uggowitzer, and J. F. Loffler, Adv. Eng. Mater. **14**, B357–B364 (2012).
[6]X. Qin, Z. Zhu, H. Fu, A. Wang, H. Zhang, and H. Zhang, J. Mater. Sci. Technol. **34**, 2290–2296 (2018).
[7]E. R. Kinser, J. Padmanabhan, R. Yu, S. L. Corona, J. Y. Li, S. Vaddiraju, A. Legassey, A. Loye, J. Balestrini, D. A. Solly, J. Schroers, A. D. Taylor, F. Padimitrakopoulos, R. Herzog, and T. R. Kyriakides, ACS Sens. **2**(12), 1779–1787 (2017).
[8]J. Dong, M. Gao, Y. Huan, Y. H. Feng, W. Liu, and W. H. Wang, J. Alloys Compd. **727**, 297–303 (2017).
[9]Z. Fan, J. Ding, and E. Ma, Mater. Res. Lett. **6**(10), 570–583 (2018).
[10]H. K. Kim, J. P. Ahn, B. J. Lee, K. W. Park, and J. C. Lee, Acta Mater. **157**, 209–217 (2018).
[11]J. Orava, I. Kaban, M. Benkocka, X. J. Han, I. Soldatov, and A. L. Greer, Thermochim. Acta **677**, 198–205 (2019).
[12]G. H. Beall, Annu. Rev. Mater. Sci. **22**, 91–119 (1992).
[13]W. Höland and G. W. Beall, *Glass-Ceramic Technology*, 2nd ed. (John Wiley & Sons Inc., Hoboken, New Jersey, 2012).
[14]Y. Kawamura, T. Shibata, A. Inoue, and T. Masumoto, Acta Mater. **46**(1), 253–263 (1998).
[15]A. Wiest, J. S. Harmon, M. D. Demetriou, R. Dale Conner, and W. L. Johnson, Scr. Mater. **60**(3), 160–163 (2009).
[16]R. Martinez, G. Kumar, and J. Schroers, Scr. Mater. **59**(2), 187–190 (2008).
[17]J. Schroers, Q. Pham, A. Peker, N. Paton, and R. V. Curtis, Scr. Mater. **57**(4), 341–344 (2007).
[18]G. Duan, A. Wiest, M. L. Lind, J. Li, W. K. Rhim, and W. L. Johnson, Adv. Mater. **19**(23), 4272 (2007).
[19]G. Kumar, P. A. Staffier, J. Blawzdziewicz, U. D. Schwarz, and J. Schroers, Appl. Phys. Lett. **97**(10), 101907 (2010).
[20]Z. Liu, N. J. Liu, and J. Schroers, Prog. Mater. Sci. **125**, 100891 (2022).
[21]R. M. Ojeda Mota, N. J. Liu, S. A. Kube, J. Chay, H. D. McClintock, and J. Schroers, Appl. Mater. Today **19**, 100567 (2020).
[22]S. D. Thakore, A. Sood, and A. K. Bansal, Drug Dev. Res. **81**(1), 3–22 (2020).
[23]D. Turnbull, Contemp. Phys. **10**(5), 473–488 (1969).
[24]A. Inoue, Acta Mater. **48**(1), 279–306 (2000).
[25]A. Takeuchi and A. Inoue, Mater. Trans. **46**(12), 2817–2829 (2005).
[26]S. Y. Ding, Y. H. Liu, Y. L. Li, Z. Liu, S. Sohn, F. J. Walker, and J. Schroers, Nat. Mater. **13**(5), 494–500 (2014).
[27]M. X. Li, S. F. Zhao, Z. Lu, A. Hirata, P. Wen, H. Y. Bai, M. W. Chen, J. Schroers, Y. H. Liu, and W. H. Wang, Nature **569**(7754), 99–103 (2019).
[28]L. Ward, S. C. O'Keeffe, J. Stevick, G. R. Jelbert, M. Aykol, and C. Wolverton, Acta Mater. **159**, 102–111 (2018).
[29]X. D. Liu, X. Li, Q. F. He, D. D. Liang, Z. Q. Zhou, J. L. Ma, Y. Yang, and J. Shen, Acta Mater. **201**, 182–190 (2020).
[30]Z. J. Li, Z. L. Long, S. Lei, T. Zhang, X. W. Liu, and D. M. Kuang, Comput. Mater. Sci. **197**, 110656 (2021).
[31]G. Liu, S. Sohn, S. A. Kube, A. Raj, A. Mertz, A. Nawano, A. Gilbert, M. D. Shattuck, C. S. O'Hern, and J. Schroers, Acta Mater. **243**, 118497 (2023).
[32]R. Dai, A. K. Gangopadhyay, R. J. Chang, and K. F. Kelton, Acta Mater. **172**, 1–5 (2019).
[33]R. Dai, R. Ashcraft, A. K. Gangopadhyay, and K. F. Kelton, J. Non-Cryst. Solids **525**, 119673 (2019).
[34]D. C. Van Hoesen, A. K. Gangopadhyay, G. Lohofer, M. E. Sellers, C. E. Pueblo, S. Koch, P. K. Galenko, and K. F. Kelton, Phys. Rev. Lett. **123**, 226601 (2019).
[35]D. M. Herlach, R. F. Cochrane, I. Egry, H. J. Fecht, and A. L. Greer, Int. Mater. Rev. **38**, 273–347 (1993).
[36]K. F. Kelton and A. Greer, *Nucleation in Condensed Matter—Applications in Materials and Biology*, 1st ed. (Elsevier, Amsterdam, 2010).
[37]J. K. R. Weber, D. S. Hampton, D. R. Merkley, C. A. Rey, M. M. Zatarski, and P. C. Nordine, Rev. Sci. Instrum. **65**, 456–465 (1994).
[38]J. K. R. Weber, C. J. Benmore, L. B. Sikinner, J. Neuefeind, S. K. Tumber, G. Jennings, L. J. Santodonato, D. Jin, J. Du, and J. B. Parise, J. Non-Cryst. Solids **383**, 49–51 (2014).
[39]W.-K. Rhim, S. K. Chung, D. Barber, K. F. Man, G. Gutt, A. Rulison, and R. E. Spjut, Rev. Sci. Instrum. **64**(10), 2961–2970 (1993).
[40]A. J. Rulison, J. L. Watkins, and B. Zambrano, Rev. Sci. Instrum. **68**(7), 2856–2863 (1997).
[41]*Metallurgy in Space*, The Mineral, Metals and Materials Society (Springer Nature, Cham, 2022).
[42]D. M. Matson, X. Xiao, J. E. Rodriguez, and R. K. Wunderlich, Int. J. Microgravity Sci. Appl. **33**(2), 330206 (2016).
[43]D. M. Herlach, S. Burggraf, P. Galenko, C. A. Gandin, A. Garcia-Escorial, H. Henein, C. Karrasch, A. Mullis, M. Rettenmayr, and J. Valloton, JOM J. Miner. Met. Mater. Soc. **69**(8), 1303–1310 (2017).
[44]M. Mohr and H.-J. Fecht, Adv. Eng. Mater. **23**(2), 2001223 (2021).

[45]R. K. Wunderlich, H. J. Fecht, and R. Willnecker, Appl. Phys. Lett. **62**(24), 3111–3113 (1993).
[46]I. Egry, G. Lohöfer, E. Gorges, and G. Jacobs, J. Phys.: Condens. Matter. **8**, 9363–9368 (1996).
[47]C. W. Morton, W. H. Hofmeister, R. J. Bayuzick, A. J. Rulison, and J. L. Watkins, Acta Mater. **46**(17), 6033–6039 (1998).
[48]I. Egry, J. Non-Cryst. Solids **250–252**, 63–69 (1999).
[49]B. Damaschke and K. Samwer, Appl. Phys. Lett. **75**(15), 2220 (1999).
[50]D. M. Herlach, J. Phys.: Condens. Matter. **13**(34), 7737 (2001).
[51]D. M. Herlach, D. Holland-Moritz, R. Willnecker, D. Herlach, and K. Maier, Philos. Trans. R. Soc. London A **361**, 497–515 (2003).
[52]R. K. Wunderlich and H.-J. Fecht, Meas. Sci. Technol. **16**, 402–416 (2005).
[53]W. K. Rhim, S. K. Chung, A. J. Rulison, and R. E. Spjut, Int. J. Thermophys. **18**(2), 459 (1997).
[54]M. B. Robinson, D. Li, J. R. Rogers, R. W. Hyers, L. Savage, and T. J. Rathz, Appl. Phys. Lett. **77**(20), 3266 (2000).
[55]Y. S. Sung, H. Takeya, and K. Togano, Rev. Sci. Instrum. **72**(12), 4419 (2001).
[56]K. F. Kelton, G. W. Lee, A. K. Gangopadhyay, R. W. Hyers, T. J. Rathz, J. R. Rogers, M. B. Robinson, and D. S. Robinson, Phys. Rev. Lett. **90**(19), 195504 (2003).
[57]S. Mukherjee, J. Schroers, Z. Zhou, W. L. Johnson, and W. K. Rhim, Acta Mater. **52**(12), 3689–3695 (2004).
[58]S. Mukherjee, W. L. Johnson, and W. K. Rhim, Appl. Phys. Lett. **86**, 014104 (2005).
[59]P. F. Paradis, T. Ishikawa, R. Fujii, and S. Yoda, Appl. Phys. Lett. **86**(4), 041901 (2005).
[60]P. F. Paradis, T. Ishikawa, and S. Yoda, J. Appl. Phys. **97**(5), 053506 (2005).
[61]R. C. Bradshaw, A. D. Arsenault, R. W. Hyers, J. R. Rogers, T. J. Rathz, G. W. Lee, A. K. Gangopadhyay, and K. F. Kelton, Philos. Mag. **86**(3–5), 341–347 (2006).
[62]R. W. Hyers and J. R. Rogers, High Temp. Mater. Proces. **27**(6), 461–474 (2008).
[63]J. C. Bendert, A. K. Gangopadhyay, N. A. Mauro, and K. F. Kelton, Phys. Rev. Lett. **109**, 185901 (2012).
[64]A. K. Gangopadhyay, J. C. Bendert, J. C. Mauro, and K. F. Kelton, J. Phys.: Condens. Matter **24**(37), 375102 (2012).
[65]J. C. Bendert, M. Blodgett, A. K. Gangopadhyay, and K. F. Kelton, Appl. Phys. Lett. **102**, 211913 (2013).
[66]T. Schenk, D. Holland-Moritz, V. Simonet, R. Bellissent, and D. M. Herlach, Phys. Rev. Lett. **89**(7), 075507 (2002).
[67]G. W. Lee, A. K. Gangopadhyay, K. F. Kelton, R. W. Hyers, T. J. Rathz, J. R. Rogers, and D. S. Robinson, Phys. Rev. Lett. **93**, 037802 (2004).
[68]D. Holland-Moritz, T. Schenk, V. Simonet, R. Bellissent, P. Convert, T. Hansen, and D. M. Herlach, Mater. Sci. Eng. A **375**, 98 (2004).
[69]T. H. Kim, G. W. Lee, B. Sieve, A. K. Gangopadhyay, R. W. Hyers, T. J. Rathz, J. R. Rogers, D. S. Robinson, K. F. Kelton, and A. I. Goldman, Phys. Rev. Lett. **95**(8), 085501 (2005).
[70]T. H. Kim and K. F. Kelton, J. Chem. Phys. **126**(5), 054513 (2007).
[71]Y. T. Shen, T. H. Kim, A. K. Gangopadhyay, and K. F. Kelton, Phys. Rev. Lett. **102**(5), 057801 (2009).
[72]N. A. Mauro, V. Wessels, J. C. Bendert, S. Klein, A. K. Gangopadhyay, M. J. Kramer, S. G. Hao, G. E. Rustan, A. Kreyssig, A. I. Goldman, and K. F. Kelton, Phys. Rev. B **83**(18), 184109 (2011).
[73]A. K. Gangopadhyay, M. E. Blodgett, M. L. Johnson, J. McKnight, V. Wessels, A. J. Vogt, N. A. Mauro, J. C. Bendert, R. Soklaski, L. Yang, and K. F. Kelton, J. Chem. Phys. **140**(4), 044505 (2014).
[74]A. K. Gangopadhyay, M. E. Blodgett, M. L. Johnson, A. J. Vogt, N. A. Mauro, and K. F. Kelton, Appl. Phys. Lett. **104**, 191907 (2014).
[75]M. L. Johnson, N. A. Mauro, A. J. Vogt, M. E. Blodgett, C. Pueblo, and K. F. Kelton, J. Non-Cryst. Solids **405**, 211–218 (2014).
[76]D. Holland-Moritz, S. Stuber, H. Hartmann, T. Unruh, T. Hansen, and A. Meyer, Phys. Rev. B **79**(6), 064204 (2009).
[77]T. Kordel, D. Holland-Moritz, F. Yang, J. Peters, T. Unruh, T. Hansen, and A. Meyer, Phys. Rev. B **83**(10), 104205 (2011).
[78]J. Brillo, A. I. Pommrich, and A. Meyer, Phys. Rev. Lett. **107**, 165902 (2011).
[79]D. Holland-Moritz, F. Yang, T. Kordel, S. Klein, F. Kargl, J. Gegner, T. Hansen, J. Bednarcik, I. Kaban, O. Shuleshova, N. Mattern, and A. Meyer, Europhys. Lett. **100**(5), 56002 (2012).
[80]S. Klein, D. Holland-Moritz, D. M. Herlach, N. A. Mauro, and K. F. Kelton, Europhys. Lett. **102**, 36001 (2013).
[81]R. Dai, J. C. Neuefeind, D. G. Quirinale, and K. F. Kelton, J. Chem. Phys. **152**, 164503 (2020).
[82]A. Meyer, S. Stuber, D. Holland-Moritz, O. Heinen, and T. Unruh, Phys. Rev. B **77**, 092201 (2008).
[83]D. Holland-Moritz, S. Stueber, H. Hartmann, T. Unruh, T. Hansen, and A. Meyer, Phys. Rev. B **79**, 064204 (2009).
[84]R. Ashcraft, Z. Wang, D. L. Abernathy, D. G. Quirinale, T. Egami, and K. F. Kelton, J. Chem. Phys. **152**(7), 074506 (2020).
[85]G. Lohofer, Rev. Sci. Instrum. **89**(12), 124709 (2018).
[86]G. Tarjus, S. A. Kivelson, Z. Nussinov, and P. Viot, J. Phys.: Condens. Matter. **17**, R1143–R1182 (2005).
[87]J. C. Dyre, Rev. Mod. Phys. **78**(3), 953–972 (2006).
[88]V. Lubchenko and P. G. Wolynes, Annu. Rev. Phys. Chem. **58**, 235–266 (2007).
[89]T. V. Tropin, J. W. P. Schmelzer, and V. L. Aksenov, Physics-USPEKHI **59**(1), 42–66 (2016).
[90]T. Egami, J. Met. **62**(2), 70–75 (2010).
[91]C. A. Angell, paper presented at the Relaxation in Complex Systems, Springfield, VA, 1984.
[92]C. A. Angell, Science **267**(5206), 1924–1935 (1995).
[93]R. Busch, J. Schroers, and W. H. Wang, MRS Bull. **32**(8), 620–623 (2007).
[94]R. Busch, E. Bakke, and W. L. Johnson, Acta Mater. **46**, 4725–4732 (1998).
[95]O. N. Senkov, Phys. Rev. B **76**(10), 104202 (2007).
[96]L. M. Wang, Y. J. Tian, and R. P. Liu, Appl. Phys. Lett. **97**(18), 181901 (2010).
[97]W. L. Johnson, J. H. Na, and M. D. Demetriou, Nat. Commun. **7**, 10313 (2016).
[98]R. Böhmer, K. L. Ngai, C. A. Angell, and D. J. Plazek, J. Chem. Phys. **99**(5), 4201–4209 (1993).
[99]M. E. Blodgett, T. Egami, Z. Nussinov, and K. F. Kelton, Sci. Rep. **5**, 13837 (2015).
[100]J. C. Mauro, Y. Yue, A. J. Ellison, P. K. Gupta, and D. C. Allan, Proc. Natl. Acad. Sci. U.S.A. **106**, 19780–19784 (2009).
[101]H. Vogel, Phys. Z. **22**, 645–646 (1921).
[102]G. S. Fulcher, J. Am. Ceram. Soc. **8**(6), 339–355 (1925).
[103]G. Tammann and W. Hesse, Z. Anorg. Allg. Chem. **156**(4), 245 (1926).
[104]G. Adam and J. H. Gibbs, J. Chem. Phys. **43**(1), 139–146 (1965).
[105]J. H. Gibbs and A. DiMarzio, J. Chem. Phys. **28**(3), 373–383 (1958).
[106]D. Turnbull and M. H. Cohen, J. Chem. Phys. **52**(6), 3038–3041 (1970).
[107]D. Turnbull and M. H. Cohen, J. Chem. Phys. **34**(1), 120–125 (1961).
[108]M. H. Cohen and D. Turnbull, J. Chem. Phys. **31**(5), 1164–1169 (1959).
[109]I. M. Hodge, J. Non-Cryst. Solids **202**, 164–172 (1996).
[110]R. Richert and C. A. Angell, J. Chem. Phys. **108**(21), 9016–9026 (1998).
[111]A. K. Gangopadhyay, C. E. Pueblo, R. Dai, M. L. Johnson, R. Ashcraft, D. Van Hoesen, M. Sellers, and K. F. Kelton, J. Chem. Phys. **146**(15), 154506 (2017).
[112]L. M. Martinez and C. A. Angell, Nature **410**(6829), 663–667 (2001).
[113]J. Ding, Y.-Q. Cheng, H. Sheng, and E. Ma, Phys. Rev. B **85**(6), 060201–060205 (2012).
[114]W. H. Wang, J. Appl. Phys. **99**(9), 093506 (2006).
[115]M. Jiang and L. Dai, Phys. Rev. B **76**(5), 054204 (2007).
[116]T. Iwashita, D. M. Nicholson, and T. Egami, Phys. Rev. Lett. **110**(20), 205504 (2013).
[117]R. C. Bradshaw, M. E. Warren, J. R. Rogers, T. J. Rathz, A. K. Gangopadhyay, K. F. Kelton, and R. W. Hyers, Ann. N. Y. Acad. Sci. **1077**, 63–74 (2006).

[118]D. Kivelson, S. A. Kivelson, X. Zhao, Z. Nussinov, and G. Tarjus, Physica A **219**, 27–38 (1995).
[119]Z. Nussinov, Phys. Rev. B **69**, 014208 (2004).
[120]Z. Evenson, T. Schmitt, M. Nicola, I. Gallino, and R. Busch, Acta Mater. **60**, 4712–4719 (2012).
[121]N. B. Weingartner, F. Nogueira, C. Pueblo, K. F. Kelton, and Z. Nussinov, Front. Mater. **3**(UNSP), 50 (2016).
[122]A. Jaiswal, T. Egami, K. F. Kelton, K. S. Schweizer, and Y. Zhang, Phys. Rev. Lett. **117**, 205701 (2016).
[123]N. Novikov, Chem. Phys. Lett. **659**, 133–136 (2016).
[124]J. M. Ziman, Philos. Mag. **6**(68), 1013–1034 (1961).
[125]C. C. Bradley, T. E. Faber, J. M. Ziman, and E. G. Wilson, Philos. Mag. **7**(77), 865 (1962).
[126]T. E. Faber and J. M. Ziman, Philos. Mag. **11**(209), 153 (1965).
[127]T. E. Faber, Adv. Phys. **15**(60), 547 (1966).
[128]A. K. Gangopadhyay and K. F. Kelton, private communication (15 December 2022).
[129]K. Ito, C. T. Moynihan, and C. A. Angell, Nature **398**(6727), 492–495 (1999).
[130]G. N. Greaves, M. C. Wilding, S. Fearn, D. Langstaff, F. Kargl, S. Cox, Q. V. Van, O. Majerus, C. J. Benmore, R. K. Weber, C. M. Martin, and L. Hennet, Science **322**(5901), 566–570 (2008).
[131]T. D. Bennett, J. C. Tan, Y. Z. Yue, E. Baxter, C. Ducati, N. J. Terrill, H. H. M. Yeung, Z. F. Zhou, W. L. Chen, S. Henke, A. K. Cheetham, and G. N. Greavves, Nat. Commun. **6**, 8079 (2015).
[132]S. Wei, F. Yang, J. Bednarcik, I. Kaban, O. Shuleshova, A. Meyer, and R. Busch, Nat. Commun. **4**, 2083 (2013).
[133]S. Lan, M. Blodgett, K. F. Kelton, J. L. Ma, J. Fan, and X.-L. Wang, Appl. Phys. Lett. **108**, 211907 (2016).
[134]H. W. Sheng, H. Z. Liu, Y. Q. Cheng, J. Wen, P. L. Lee, W. K. Luo, S. D. Shastri, and E. Ma, Nat. Mater. **6**(3), 192–197 (2007).
[135]H. W. Luan, X. Zhang, H. Y. Ding, F. Zhang, J. H. Luan, Z. B. Jiao, Y. C. Yang, H. T. Bu, R. B. Wang, J. L. Gu, C. L. Shao, Q. Yu, Y. Shao, Q. Zeng, N. Chen, C. T. Liu, and K. F. Yao, Nat. Commun. **13**(1), 2183 (2022).
[136]J. Shen, Y. Sun, J. Orava, H. Y. Bai, and W. H. Wang, Acta Mater. **225**, 117588 (2022).
[137]W. Xu, M. T. Sandor, Y. Yu, H. B. Ke, H. P. Zhang, M. Z. Li, W. H. Wang, L. Liu, and Y. Wu, Nat. Commun. **6**, 7696 (2015).
[138]X. Zhao, C. Z. Wang, H. J. Zheng, Z. A. Tian, and L. N. Hu, Phys. Chem. Chem. Phys. **19**(24), 15962–15972 (2017).
[139]M. Stolpe, I. Jonas, S. Wei, Z. Evenson, W. Hembree, F. Yang, A. Meyer, and R. Busch, Phys. Rev. B **93**(1), 014201 (2016).
[140]I. Saika-Voivod, P. H. Poole, and F. Sciortino, Nature **412**(6846), 514–517 (2001).
[141]M. Hemmati, C. T. Moynihan, and C. A. Angell, J. Chem. Phys. **115**(14), 6663–6671 (2001).
[142]S. Harrington, R. J. Zhang, P. H. Poole, F. Sciortino, and H. E. Stanley, Phys. Rev. Lett. **78**(12), 2409–2412 (1997).
[143]J. N. Glosli and F. H. Ree, Phys. Rev. Lett. **82**(23), 4659–4662 (1999).
[144]C. Z. Zhang, L. N. Hu, Y. Z. Yue, and J. C. Mauro, J. Chem. Phys. **133**(1), 014508 (2010).
[145]C. Zhou, L. N. Hu, Q. J. Sun, H. J. Zheng, C. Z. Zhang, and Y. Z. Yue, J. Chem. Phys. **142**(6), 064508 (2015).
[146]X. T. Zhai, X. Li, Z. Wang, L. N. Hu, K. K. Song, Z. Tian, and Y. Yue, Acta Mater. **239**, 118246 (2022).
[147]J. J. Z. Li, W. K. Rhim, C. P. Kim, K. Samwer, and W. L. Johnson, Acta Mater. **59**, 2166–2171 (2011).
[148]E. A. Jagla, J. Phys.: Condes. Matter **11**(50), 10251–10258 (1999).
[149]L. Liu, S. H. Chen, A. Faraone, C. W. Yen, and C. Y. Mou, Phys. Rev. Lett. **95**(11), 117802 (2005).
[150]J. Hedström, J. Swenson, R. Bergman, H. Jansson, and S. Kittaka, Eur. Phys. J. Spec. Top. **141**, 53–56 (2007).
[151]H. Tanaka, J. Phys.: Condens. Matter **15**(45), L703–L711 (2003).
[152]Q. J. Sun, C. Zhou, Y. Z. Yue, and L. N. Hu, J. Phys. Chem. Lett. **5**(7), 1170–1174 (2014).
[153]F. Z. Chen, N. A. Mauro, S. M. Bertrand, P. McGrath, L. Zimmer, and K. F. Kelton, J. Chem. Phys. **155**, 104501 (2021).
[154]N. Mattern, H. Hermann, S. Roth, J. Sakowski, M.-P. Macht, P. Jovari, and J. Z. Jiang, Appl. Phys. Lett. **82**(16), 2589–2591 (2003).
[155]K. Georgarakis, D. V. Louzguine-Luzgin, J. Antonowicz, G. Vaughan, A. R. Yavari, T. Egami, and A. Inoue, Acta Mater. **59**(2), 708–716 (2011).
[156]H. Lou, X. Wang, Q. Cao, D. Zhang, T. Hu, H. Mao, and J.-Z. Jiang, Proc. Natl. Acad. Sci. U.S.A. **110**(25), 10068–10072 (2013).
[157]P. Ehrenfest, Proc. K. Ned. Akad. Wet. **17**, 1184–1190 (1915).
[158]A. K. Gangopadhyay and K. F. Kelton, J. Chem. Phys. **148**(20), 204509 (2018).
[159]J. Ding, M. Xu, P. F. Guan, S. W. Deng, Y. Q. Cheng, and E. Ma, J. Chem. Phys. **140**(6), 064501 (2014).
[160]J. Ding and E. Ma, NPJ Comput. Mater. **3**, 9 (2017).
[161]S. V. Sukhomlinov and M. H. Muser, J. Chem. Phys. **146**, 024506 (2017).
[162]R. Ashcraft and K. F. Kelton, arXiv:1810.08889 [cond-mat.mtrl-sci] (2018).
[163]R. L. McGreevy and P. Zetterstrom, J. Non-Cryst. Solids **293–295**(0), 297–303 (2001).
[164]R. L. McGreevy, J. Phys.: Condens. Matter **13**, R877–R913 (2001).
[165]R. L. McGreevy and J. D. Wicks, J. Non-Cryst. Solids **192–193**, 23–27 (1995).
[166]R. L. McGreevy, Nucl. Instrum. Methods Phys. Res. Sect. A **354**, 1–16 (1995).
[167]R. L. McGreevy, J. Non-Cryst. Solids **156–158**(Part 2 (0)), 949–955 (1993).
[168]M. L. McGreevy, J. Phys.: Condens. Matter **3**, F9–F22 (1991).
[169]K.-Y. Ahn, D. Louca, S. J. Poon, and G. J. Shiflet, Phys. Rev. B **70**(22), 224103 (2004).
[170]D. Ma, A. D. Stoica, L. Yang, X.-L. Wang, Z. P. Lu, J. Neuefeind, M. J. Kramer, J. W. Richardson, and T. Proffen, Appl. Phys. Lett. **90**, 211908 (2007).
[171]P. S. Salmon and A. Zeidler, Phys. Chem. Chem. Phys. **15**(37), 15286–15308 (2013).
[172]M. L. Johnson, M. E. Blodgett, K. A. Lokshin, N. A. Mauro, J. Neuefeind, C. Pueblo, D. G. Quirinale, A. J. Vogt, T. Egami, A. I. Goldman, and K. F. Kelton, Phys. Rev. B **93**, 054203 (2016).
[173]J. D. Honeycutt and H. C. Andersen, J. Phys. Chem. **91**, 4950 (1987).
[174]Y.-Q. Cheng and E. Ma, Prog. Mater. Sci. **56**, 379–473 (2011).
[175]J. L. Finney, Proc. R. Soc. Lond. A **319**(1539), 479–493 (1970).
[176]J. L. Finney, Nature **266**(5600), 309–314 (1977).
[177]F. Puosi and A. Pasturel, Acta Mater. **174**, 387–397 (2019).
[178]Y. Q. Cheng, E. Ma, and H. W. Sheng, Appl. Phys. Lett. **93**(11), 111913 (2008).
[179]F. Puosi, N. Jakse, and A. Pasturel, J. Phys.: Condens. Matter **30**(14), 145701 (2018).
[180]C. H. Bennett, D. E. Polk, and D. Turnbull, Acta Metall. **19**(12), 1295–1298 (1971).
[181]P. Bordat, F. Affouard, M. Descamps, and K. L. Ngai, Phys. Rev. Lett. **93**(10), 105502 (2004).
[182]D. Reith, M. Putz, and F. Muller-Plathe, J. Comput. Chem. **24**(13), 1624–1636 (2003).
[183]J. P. Hansen and I. R. McDonald, *Theory of Simple Liquids* (Elsevier Ltd, 1990).
[184]J. Krausser, K. H. Samwer, and A. Zaccone, Proc. Natl. Acad. Sci. U.S.A. **112**(45), 13762–13767 (2015).
[185]R. D. Shannon, Acta Crystallogr. **32**(SEP1), 751–767 (1976).
[186]C. E. Pueblo, M. Sun, and K. F. Kelton, Nat. Mater. **16**(8), 792–796 (2017).
[187]T. Egami, Front. Phys. **8**, 50 (2020).
[188]N. A. Mauro, M. Blodgett, M. L. Johnson, A. J. Vogt, and K. F. Kelton, Nat. Commun. **5**, 4616 (2014).
[189]S. Wei, M. Stolpe, O. Gross, Z. Evenson, I. Gallino, W. Hembree, J. Bednarcik, J. J. Kruzic, and R. Busch, Appl. Phys. Lett. **106**, 181901 (2015).
[190]S. Chakrabarty and Z. Nussinov, Phys. Rev. B **84**(6), 064124 (2011).

[191]C. W. Ryu, W. Dmowski, K. F. Kelton, G. W. Lee, E. S. Park, J. R. Morris, and T. Egami, Sci. Rep. **9**, 18579 (2019).
[192]B. Wu, T. Iwashita, and T. Egami, Phys. Rev. E **92**(5), 052303 (2015).
[193]C. W. Ryu and T. Egami, Phys. Rev. E **102**, 042615 (2020).
[194]M. X. Li, Y. T. Sun, C. Wang, L. W. Hu, S. Sohn, J. Schroers, W. H. Wang, and Y. H. Liu, Nat. Mater. **21**(2), 165 (2022).
[195]L. S. Ornstein and F. Zernike, Proc. K. Ned. Akad. Wet. **17**, 793–806 (1914).
[196]S. Wei, Z. Evenson, I. Gallino, and R. Busch, Intermetallics **55**, 138–144 (2014).
[197]S. A. Kube, S. Sohn, R. Ojeda-Mota, T. Evers, W. Polsky, N. J. Liu, K. Ryan, S. Rinehart, Y. Sun, and J. Schroers, Nat. Commun. **13**(1), 3708 (2022).
[198]L. Van Hove, Phys. Rev. **95**(1), 249–262 (1954).
[199]J. N. Roux, J. L. Barrat, and J.-P. Hansen, J. Phys.: Condens. Matter. **1**, 7171–7186 (1989).
[200]W. Kob and H. C. Andersen, Phys. Rev. E **52**(4), 4134–4153 (1995).
[201]R. Yamamoto and A. Onuki, Phys. Rev. Lett. **81**(22), 4915–4918 (1998).
[202]U. Dahlborg, W. Gudowski, and M. Davidovic, J. Phys.: Condens. Matter **1**(35), 6173–6179 (1989).
[203]T. Iwashita, B. Wu, W.-R. Chen, S. Tsutsui, A. Q. R. Baron, and T. Egami, Sci. Adv. **3**(12), e1603079 (2017).
[204]Y. Shinohara, W. Dmowski, T. Iwashita, B. Wu, D. Ishikawa, A. Q. R. Baron, and T. Egami, Phys. Rev. E **98**, 022604 (2018).
[205]T. E. Mason, D. L. Abernathy, I. Anderson, J. Ankner, T. Egami, G. Ehlers, A. Ekkebus, G. Granroth, M. Hagen, K. Herwig, J. Hodges, C. Hoffmann, C. Horak, L. Horton, F. Klose, J. Larese, A. Mesecar, D. Myles, J. Neuefeind, M. Ohl, C. Tulk, X. L. Wang, and J. Zhao, Physica B **385–386**, 955–960 (2006).
[206]N. A. Mauro, A. J. Vogt, K. S. Derendorf, M. L. Johnson, G. E. Rustan, D. G. Quirinale, A. Kreyssig, K. A. Lokshin, J. C. Neuefeind, K. An, X. L. Wang, A. I. Goldman, T. Egami, and K. F. Kelton, Rev. Sci. Instrum. **87**(1), 013904 (2016).
[207]B. Wu, T. Iwashita, and T. Egami, Phys. Rev. Lett. **120**, 135502 (2018).
[208]A. L. Greer, Science **267**(5206), 1947–1953 (1995).
[209]C. Suryanarayana and A. Inoue, *Bulk Metallic Glasses* (CRC Press, Taylor & Francis Group, Boca Raton, FL, 2018).
[210]A. Inoue, Acta Mater. **48**(1), 279–306 (2000).
[211]Y. L. Li, K. E. Jensen, Y. H. Liu, J. B. Liu, P. Gong, B. E. Scanley, C. C. Broadbridge, and J. Schroers, ACS Comb. Sci. **18**(10), 630–637 (2016).
[212]J. Wang, A. Agrawal, and K. Flores, Acta Mater. **171**, 163–169 (2019).
[213]W. P. Weeks and K. M. Flores, Intermetallics **145**, 107560 (2022).
[214]A. L. Greer, Nature **366**(6453), 303–304 (1993).
[215]E. Perim, D. Lee, Y. H. Liu, C. Toher, P. Gong, Y. L. Li, W. N. Simmons, O. Levy, J. J. Vlassak, J. Schroers, and S. Curtarolo, Nat. Commun. **7**, 12315 (2016).
[216]J. K. Stalick and R. M. Waterstrat, J. Alloys Compd. **430**(1–2), 123–131 (2007).
[217]J. Saida, M. Matsushita, and A. Inoue, Appl. Phys. Lett. **77**, 73–75 (2000).
[218]K. F. Kelton and A. L. Greer, in *5th International Conference on Rapidly Quenched Metals*, S. S. a. H. Warlimont (North Holland, Wurzburg, 1985), pp. 223–226.
[219]J. W. Gibbs, *Scientific Papers* (Longmans Green, London, 1906).
[220]M. Volmer and A. Weber, Z. Phys. Chem. **119**, 227–301 (1926).
[221]H. Eyring, J. Chem. Phys. **3**(2), 107–115 (1935).
[222]K. F. Kelton, in *Metallurgy in Space—Recent Results from ISS*, edited by H.-J. Fecht and M. Mohr (Springer Nature Switzerland AG and The Minerals, Metals and Materials Society, Cham, 2021), pp. 153–178.
[223]C. K. Bagdassarian and D. W. Oxtoby, J. Chem. Phys. **100**(3), 2139–2148 (1994).
[224]F. Spaepen, in *Solid State Physics*, edited by H. Ehrenreich and D. Turnbull (Academic Press, New York, 1994), Vol. 47, pp. 1–32.
[225]L. Granasy, J. Non-Cryst. Solids **162**(3), 301–303 (1993).
[226]L. Granasy, J. Non-Cryst. Solids **219**, 49–56 (1997).
[227]P. J. Desre, E. Cini, and B. Vinet, J. Non-Cryst. Solids **288**, 210–217 (2001).
[228]E. Cini, B. Vinet, and P. J. Desre, Philos. Mag. A **80**, 955–966 (2000).
[229]Z. Wang, C. Chen, S. V. Ketov, K. Akagi, A. A. Tsarkov, Y. Ikuhara, and D. V. Louzguine-Luzgin, Mater. Des. **156**, 504–513 (2018).
[230]D. Moroni, P. R. ten Wolde, and P. G. Bolhuis, Phys. Rev. Lett. **94**, 235703 (2005).
[231]F. Puosi and A. Pasturel, Phys. Rev. Mater. **3**(2), 023402 (2019).
[232]E. Wigner, Z. Phys. Chem. Abteilung B-Chem. Elementarprozesse Aufbau der Mater. **19**(2/3), 203–216 (1932).
[233]L. Zhao, G. B. Bokas, J. H. Perepezko, and I. Szlufarska, Acta Mater. **142**, 1–7 (2018).
[234]F. Z. Chen, Z. Nussinov, and K. F. Kelton, arXiv:2212.14119 (2022).
[235]F. Z. Chen, private communication (8 December 2022).
[236]F. Hou, J. D. Martin, E. D. Dill, J. C. W. Folmer, and A. A. Josey, Chem. Mater. **27**, 3526–3532 (2015).
[237]J. D. Martin, B. G. Hillis, and F. Hou, J. Phys. Chem. C **124**, 18724–18740 (2020).
[238]W. Kauzmann, Chem. Rev. **43**(2), 219–256 (1948).
[239]D. Q. M. Craig, P. G. Royall, V. L. Kett, and M. L. Hopton, Int. J. Pharm. **179**, 179–207 (1999).
[240]Y. Lin, M. M. Smedskjaer, and J. C. Mauro, Int. J. Appl. Glass Sci. **10**, 488–501 (2019).
[241]J. Zhao, S. L. Simon, and G. B. McKenna, Nat. Commun. **4**, 1783 (2013).
[242]T. Pérez-Castañeda, R. J. Jaménez-Riobóo, and M. A. Ramos, Phys. Rev. Lett. **112**, 165901 (2014).
[243]W. Klement, P. Duwez, and R. H. Willens, Nature **187**(4740), 869–870 (1960).
[244]S. F. Swallen, K. L. Kearns, M. K. Mapes, Y. S. Kim, R. J. McMahon, M. D. Ediger, T. Wu, L. Yu, and S. Satija, Science **315**, 353–356 (2007).
[245]A. Q. Tool, J. Am. Ceram. Soc. **29**(9), 240–253 (1946).
[246]C. Rodriguez-Tinoco, M. Gonzalez-Silveira, J. Rafols-Ribe, G. Garcia, and J. Rodriguez-Viejo, J. Non-Cryst. Solids **407**, 256–261 (2015).
[247]M. D. Ediger, J. Chem. Phys. **147**, 210901 (2017).
[248]C. Rodriguez-Tinco, M. Gonzalez-Silveira, M. A. Ramos, and J. Rodriguez-Viejo, La Rivista del Nuovo Cimento **45**, 325–406 (2022).
[249]H.-B. Yu, Y. Luo, and K. Samwer, Adv. Mater. **25**, 5904–5908 (2013).
[250]C. R. Cao, Y. M. Lu, H. Y. Bai, and W. H. Wang, Appl. Phys. Lett. **107**(14), 141606 (2015).
[251]D. J. Magagnosc, G. Feng, L. Yu, X. Cheng, and D. S. Gianola, APL Mater. **4**(8), 086104 (2016).
[252]P. Luo, C. R. Cao, F. Zhu, Y. M. Lv, Y. H. Liu, P. Wen, H. Y. Bai, G. Vaughan, M. di Michiel, B. Ruta, and W. H. Wang, Nat. Commun. **9**, 1389 (2018).
[253]D. V. Louzguine-Luzgin and J. Z. Jiang, Metals **9**(10), 1076 (2019).
[254]Y. Zhao, B. S. Shang, B. Zhang, X. Tong, H. B. Ke, H. Y. Bai, and W. H. Wang, Sci. Adv. **8**(33), eabn3623 (2022).
[255]R. J. Xue, L. Z. Zhao, C. L. Shi, T. Ma, X. K. Xi, M. Gao, P. W. Zhu, P. Wen, X. H. Yu, C. Q. Jin, M. X. Pan, W. H. Wang, and H. Y. Bai, Appl. Phys. Lett. **109**, 221904 (2016).
[256]T. Eckert and E. Bartsch, Phys. Rev. Lett. **89**(12), 125701 (2002).
[257]A. Crisanti and L. Leuzzi, Phys. Rev. B **73**, 014412 (2006).
[258]M. Zhu, J.-Q. Wang, J. H. Perepezko, and L. Yu, J. Chem. Phys. **142**, 244504 (2015).
[259]S. Lan, Y. Ren, X. Y. Wei, B. Wang, E. P. Gilbert, T. Shibayama, S. Watanabe, M. Ohnuma, and X.-L. Wang, Nat. Commun. **8**, 14679 (2017).
[260]Q. Du, X. Liu, H. Fan, Q. Zeng, Y. Wu, H. Wang, D. Chatterjee, Y. Ren, Y. Ke, P. M. Voyles, Z. Lu, and E. Ma, Mater. Today **34**, 66–77 (2020).
[261]L. Hu, X. Bian, W. Wang, G. Liu, and Y. Jia, J. Phys. Chem. B **109**(28), 13737–13742 (2005).
[262]J. L. Walter, F. Bacon, and F. E. Luborsky, Mater. Sci. Eng. **24**, 239–245 (1976).
[263]S. V. Ketov, Y. H. Sun, S. Nachum, Z. Lu, A. Checchi, A. R. Beraldin, H. Y. Bai, W. H. Wang, D. V. Louzguine-Luzgin, M. A. Carpenter, and A. L. Greer, Nature **524**, 200 (2015).

[264]Y. H. Sun, A. Concustell, and A. L. Greer, Nat. Rev. Mater. **1**(9), 16039 (2016).
[265]J. Pan, Y. P. Ivanov, W. H. Zhou, Y. Li, and A. L. Greer, Nature **578**(7796), 559 (2020).
[266]D. Grell, F. Dabrock, and E. Kerscher, Fatigue Fract. Eng. Mater. Struct. **41**(6), 1330–1343 (2018).
[267]B. S. Li, S. H. Xie, and J. J. Kruzic, Acta Mater. **176**, 278–288 (2019).
[268]M. Stolpe, J. J. Kruzic, and R. Busch, Acta Mater. **64**, 231–240 (2014).
[269]A. Concustell, F. O. Mear, S. Surinach, M. D. Baro, and A. L. Greer, Philos. Mag. Lett. **89**(12), 831–840 (2009).
[270]R. E. Baumer and M. J. Demkowicz, Acta Mater. **83**, 419–430 (2015).
[271]S. V. Ketov, A. S. Trifonov, Y. P. Ivanov, A. Y. Churyumov, A. V. Lubenchenko, A. A. Batrakov, J. Z. Jiang, D. V. Louzguine-Luzgin, J. Eckert, J. Orava, and A. L. Greer, NPG Asia Mater. **10**, 137–145 (2018).
[272]H. B. Lou, Z. D. Zeng, F. Zhang, S. Y. Chen, P. Luo, X. H. Chen, Y. Ren, V. B. Prakapenka, C. Prescher, X. B. Zuo, T. B. Li, J. G. Wen, W. H. Wang, H. W. Sheng, and Q. S. Zeng, Nat. Commun. **11**(1), 314 (2020).
[273]M. B. Costa, J. J. Londono, A. Blatter, A. Hariharan, A. Gebert, M. A. Carpenter, and A. L. Greer, Acta Mater. **244**, 118551 (2023).
[274]S. J. Kang, Q. P. Cao, J. Liu, Y. Tang, X. D. Wang, D. X. Zhang, I. S. Ahn, A. Caron, and J. Z. Jiang, J. Alloys Compd. **795**, 493–500 (2019).
[275]F. Bu, J. Wang, L. Y. Li, H. C. Kou, X. Y. Xue, and J. S. Li, Metals **6**(11), 274 (2016).
[276]J. Ketkaew, R. Yamada, H. Wang, D. Kuldinow, B. S. Schroers, W. Dmowski, T. Egami, and J. Schroers, Acta Mater. **184**, 100–108 (2020).
[277]H. B. Yu, W. H. Wang, and K. Samwer, Mater. Today **16**, 183–191 (2013).
[278]H. B. Yu, X. Shen, Z. Wang, L. Gu, W. H. Wang, and H. Y. Bai, Phys. Rev. Lett. **108**(1), 015504 (2012).
[279]H. B. Yu, K. Samwer, W. H. Wang, and H. Y. Bai, Nat. Commun. **4**, 2204 (2013).
[280]Y. Tong, T. Iwashita, W. Dmowski, H. Bei, Y. Yokoyama, and T. Egami, Acta Mater. **86**, 240–246 (2015).
[281]M. Samavatian, R. Gholamlpour, A. A. Amadeh, and V. Samavatian, Physica B **595**, 412390 (2020).
[282]F. Q. Meng, S. Y. Wang, and D. B. Sun, Intermetallics **121**, 106764 (2020).
[283]A. Das, E. M. Dufresne, and R. Maaß, Acta Mater. **196**, 723–732 (2020).
[284]B. Shang, W. H. Wang, A. L. Greer, and P. F. Guan, Acta Mater. **213**, 116952 (2021).
[285]A. K. Gangopadhyay, Z. Nussinov, and K. F. Kelton, Phys. Rev. E **106**(5), 054150 (2022).
[286]B. Guiselin, G. Tarjus, and L. Berthier, ArXiv:2207.14204 (2022).